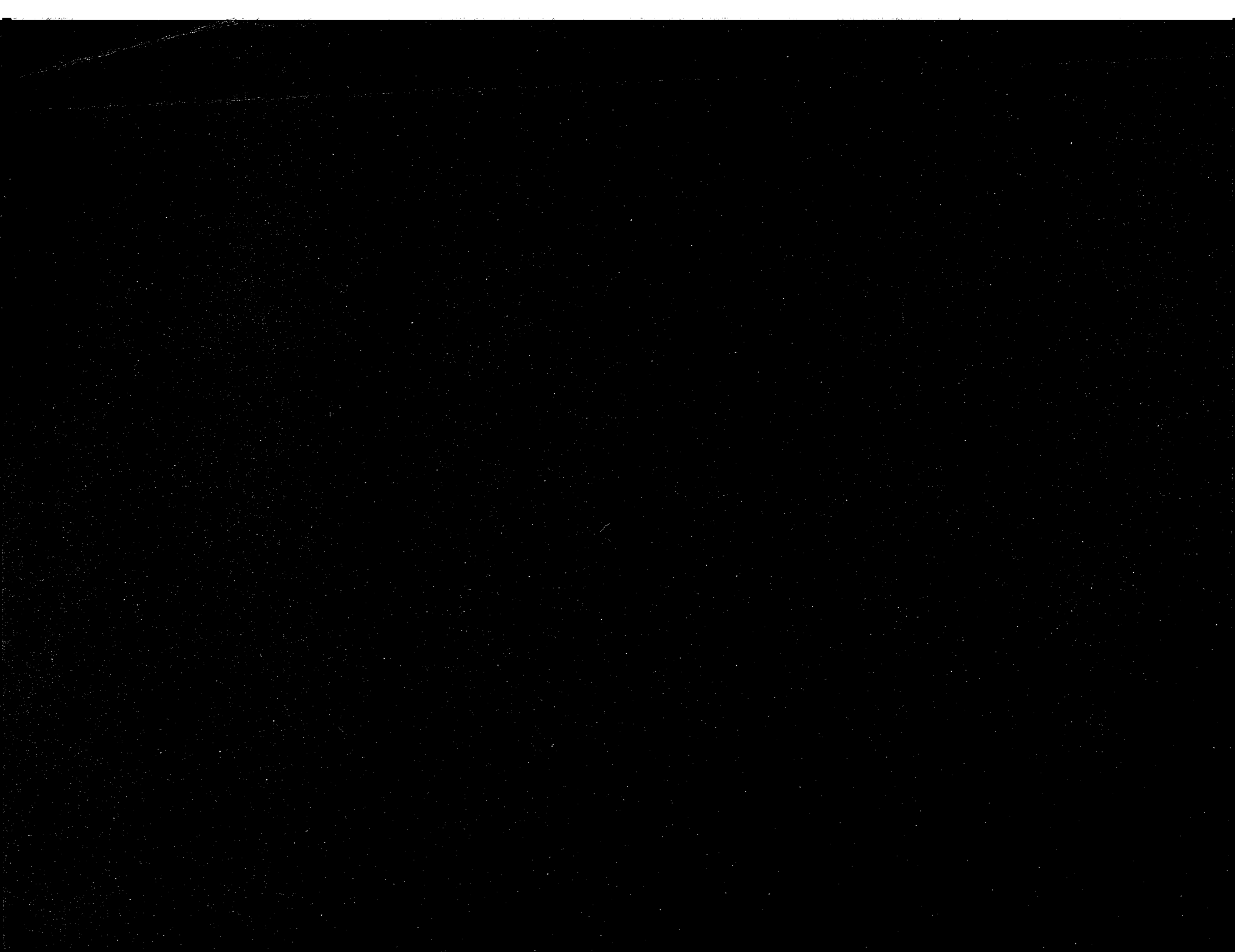

1. Report No.	2. Government Accession No.	3. Recipient's Catalog No.
NASA CR-168070		

4. Title and Subtitle	5. Report Date
Energy Efficient Engine Fan and Quarter-Stage Component Performance Report	Jan. 1983
	6. Performing Organization Code

7. Author(s)	8. Performing Organization Report No.
S.J. Cline J.T. Kutney, Jr. P.H. Halter T.J. Sullivan	R82AEB408
	10. Work Unit No.

9. Performing Organization Name and Address	11. Contract or Grant No.
General Electric Company Aircraft Engine Business Group Cincinnati, Ohio 45215	NAS3-20643
	13. Type of Report and Period Covered
12. Sponsoring Agency Name and Address	Topical
NASA - Lewis Research Center 21000 Brookpark Road Cleveland, Ohio 44135	14. Sponsoring Agency Code

15. Supplementary Notes

NASA Project Manager: Mr. C.C. Ciepluch G.E. Project Manager: R.W. Bucy
NASA Project Engineer: Mr. R.D. Hager

16. Abstract

The fan configuration for the General Electric/NASA Energy Efficient Engine was selected following an extensive preliminary design study. The fan has an inlet radius ratio of 0.342 and a specific flowrate of 208.9 Kg/sec-M^2 (42.8 lbm/sec-ft^2). The design corrected tip speed is 411.5 m/sec (1350 ft/sec) producing a bypass flow total-pressure ratio of 1.65 and a core flow total-pressure ratio of 1.67. The design bypass ratio is 6.8. The aerodynamic design point corresponds to the maximum climb power setting at Mach 0.8 and 10.67 Km (35,000 ft) altitude.

The fully-instrumented fan component was tested in the Lynn Large Fan Test Facility in 1981. The overall performance results, reported herein, showed excellent fan performance with the fan meeting all of its component test goals of flow, efficiency and stall margin.

17. Key Words (Suggested by Author(s))	18. Distribution Statement
Fan and Quarter Stage Booster Bypass Ratio Core Stream Efficiency Energy Efficient Engine	[redacted]

19. Security Classif. (of this report)	20. Security Classif. (of this page)	21. No. of Pages	22. Price*
Unclassified	Unclassified	68	

[redacted]

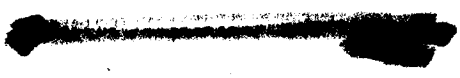

FOREWORD

This report presents the results of the full-scale fan test and data analysis performed by the General Electric Company for the National Aeronautics and Space Administration, Lewis Research Center under Contract NAS3-20643. This work was performed as part of the Aircraft Energy Efficiency Program, Energy Efficient Engine Project. Mr. C.C. Ciepluch is the NASA Project Manager and Mr. P.G. Batterton is the NASA Assistant Project Manager. Mr. R.D. Hager is the NASA Project Engineer responsible for managing the effort associated with the fan component performance and analysis presented in this report. Mr. R.W. Bucy is the Manager of the Energy Efficient Engine Project for the General Electric Company.. This report was prepared by Messrs. S.J. Cline, P.H. Halter, J.T. Kutney, Jr, and T.J. Sullivan of the General Electric Company, Evendale, Ohio.

TABLE OF CONTENTS

LIST OF ILLUSTRATIONS

LIST OF ILLUSTRATIONS (Continued)

LIST OF TABLES

SECTION I

INTRODUCTION AND SUMMARY

The fan configuration for the General Electric/NASA Energy Efficient Engine was selected following an extensive preliminary design study of alternate designs. The final design configuration, shown in Figure 1 and described in detail in Reference 1, was found to give the lowest mission fuel-burn and direct operating cost of all those studied. As shown in Figure 1, the E^3 fan configuration uses a quarter-stage booster to provide the required core supercharging. This type of design was chosen over a single-stage rotor with a higher tip speed and a more highly loaded hub because of its higher core-stream efficiency potential and its easier growth path for future engine development. The fan bypass stream also has a higher efficiency potential by reason of the lower fan speed. Additionally, the quarter-stage island arrangement provides an excellent means for separating foreign objects from the core flow.

The fan has an inlet radius ratio of 0.342 and a specific flow rate of 208.9 Kg/sec-M^2 (42.8 lbm/sec-ft^2). The design corrected tip speed is 411.5 m/sec (1350 ft/sec) producing a bypass flow total-pressure ratio of 1.65 and core flow total-pressure ratio of 1.67. The quarter-stage island splits the total fan flow so that approximately 22% of the total flow is supercharged by the quarter-stage rotor. Downstream of the booster rotor, the flow is further split with 42% of the booster flow re-entering the bypass stream and the remaining flow directed through the innner outlet guide vanes and the transition duct into the core. The aerodynamic design point corresponds to the maximum climb power setting at Mach 0.80 and 10.67 km (35,000 feet) altitude. The design bypass ratio is 6.8.

The fully-instrumented fan component was tested in the General Electric Large Fan Test Facility in Lynn, Massachusetts from September to November 1981. A total of 276 aerodynamic performance readings were taken during 81.6 hours of testing. The fan was stalled 14 times to determine the stall margin at key cycle operating conditions. Steady-state performance readings were taken on 11 speedlines from a very low operating line to near stall. Large swings in

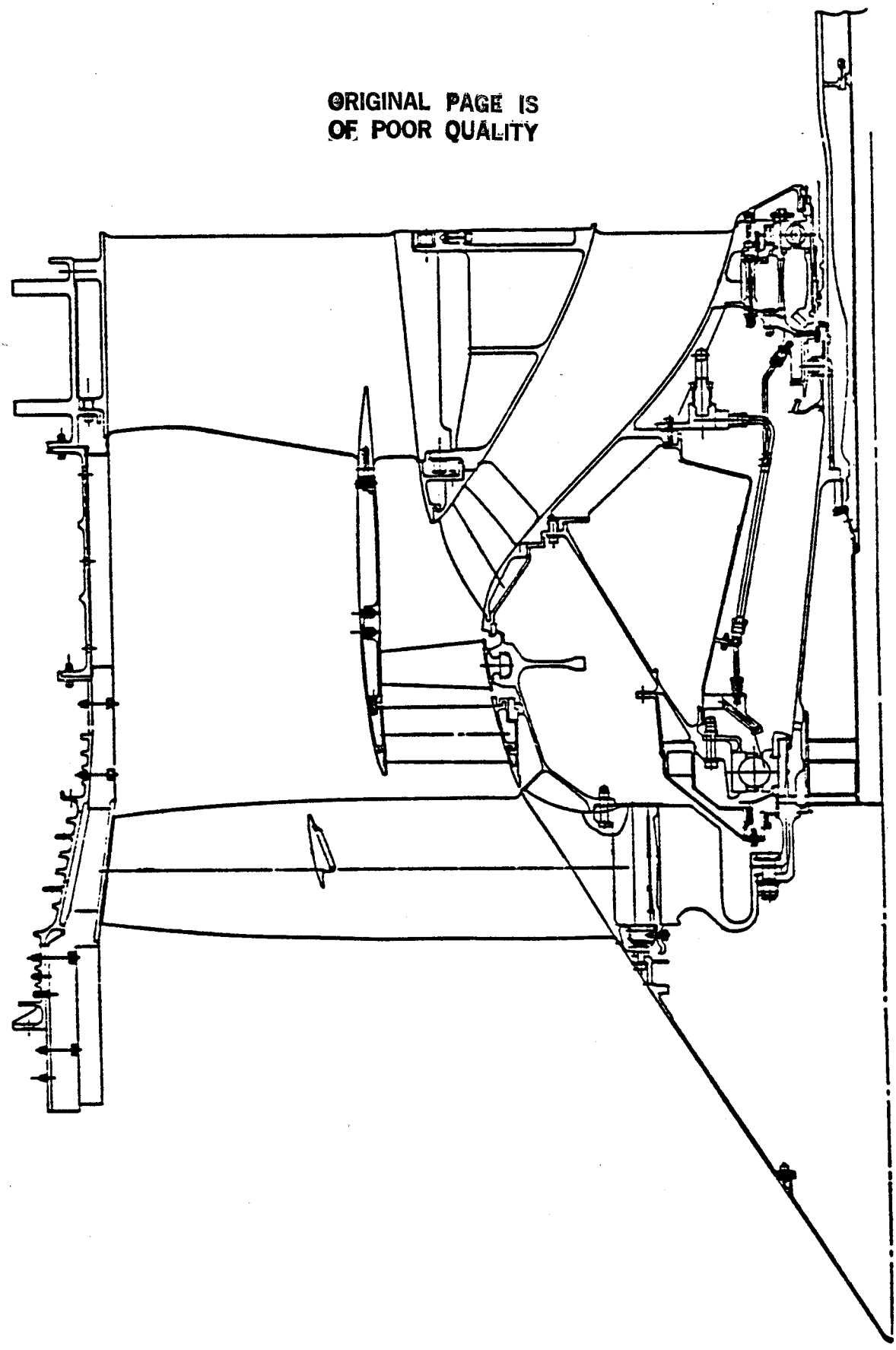

Figure 1. E^3 Fan Configuration.

bypass ratio were demonstrated at the 90% and 95% corrected speeds with steady-state readings taken at bypass ratios ranging from 4 to 13.

The overall performance results showed excellent fan performance with the fan exceeding all of its component test goals of flow, efficiency and stall margin. At the max climb aerodynamic design point, the fan bypass momentum averaged, adiabatic efficiency was 0.886, 1.7 points higher than the component goal. The measured airflow was 1.4% higher than design at 100% corrected speed; the design airflow was reached at 97.5% speed. The stall margin was 3-5% higher than the target with 15% constant-flow margin demonstrated at the takeoff condition. The core-stream mass-averaged adiabatic efficiency was between 0.890 and 0.900 all along the cruise operating line for engine-matched bypass ratios. At the maximum cruise condition, the measured core-stream adiabatic efficiency was 0.892, 1.7 points higher than the test goal. The quarter-stage stall margin was found to be adequate for stable engine operation. Rotating stalls occurred when throttling the core-stream to very high bypass ratios with the quarter-stage rotor operating approximately 10% above the predicted stall line. An unintentional stall occured at 100% speed with the fan and quarter-stage both operating near stall. The stall was found to have been caused by the quarter-stage rotor when the core-stream was throttled to a very high bypass ratio.

The vibratory response levels of the fan and quarter-stage rotor blades were very low during normal fan test operation. Normal fan operation produced a maximum fan blade response of 21 percent of limits and a quarter-stage response of only 17 percent of limits. The highest stress levels seen during a stall were 50 percent of limits for the fan blade and 65 percent of limits for the quarter-stage blade.

The fan stator airfoils also showed low stress levels throughout the fan test. The maximum percent of limits (77%) was observed on the core OGV at a speed of 3732 rpm. Below 3500 rpm, the core OGV's exhibited very little response. The bypass vane showed extremely low excitations at all fan speeds.

The full-scale fan test was completed with acceptable synchronous vibration levels throughout the entire speed range following a successful field balance of the Stage 1 fan rotor.

SECTION II

INSTRUMENTATION AND TEST CONFIGURATION

A cross-section drawing showing the design flow stream-lines of the instrumented test rig flowpath is shown in Figure 2. A cross-section of the bellmouth, inlet and exit ducts, and the test vehicle are also shown, as well as the aerodynamic instrumentation plane definition.

The main aerodynamic instrumentation planes used for defining the overall fan performance are:

Inlet Screen (Plane 2)	Twenty-four thermocouples positioned over the entire screen to provide a representative temperature sampling of the total inlet flow.
Inlet Plane (Plane 10)	Four 6-element pitot-static rakes, located at the bellmouth throat, used to measure total fan flow and inlet total pressure.
Bypass OGV exit (Plane 14)	Seven 11-element arc rakes and seven 7-element radial rakes located 1/2 chord length behind bypass OGV's.
Core OGV exit (Plane 23)	Five 11-element arc rakes located between inner OGV's and the core frame struts.

Other aerodynamic instrumentation were located on the vane leading edges, the flowpath walls, and the core duct exit (compressor inlet, Plane 25). A boundary-layer rake at the fan rotor inlet (Plane 12) was used to measure the total-pressure gradient near the outer wall and to determine the total-pressure loss in the duct between Plane 10 and Plane 12.

The fan and quarter-stage rotor blades were fully-instrumented with dynamic strain gages for the full-scale fan test. Eighteen strain gages on the fan rotor and twelve strain gages on the quarter-stage rotor were used to detect the vibration characteristics of the airfoils. Additional strain gages were placed on the Stage 1 and 2 disks and the Stage 2 spacer.

The aeromechanical performances of the fan stator vanes were obtained by the use of fifteen dynamic strain gages per stage. Three of these gages were used as spares and the remaining twelve were monitored on scopes and simultaneously recorded on magnetic tape. The locations of these gages are listed

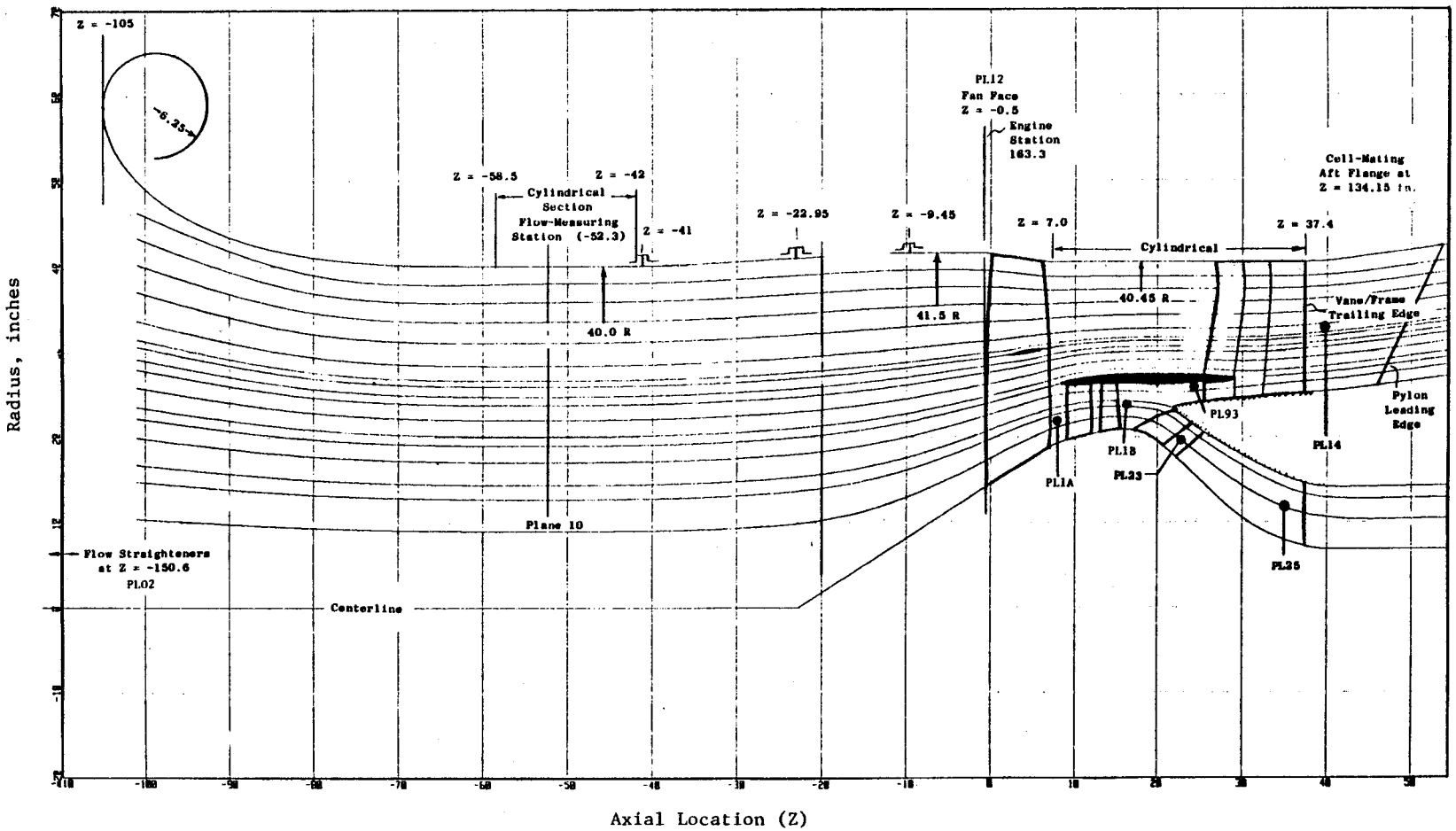

Figure 2. Fan Component Test-Rig Flowpath.

in Table I. Three of the core OGV gages were lost during vehicle build-up. A total of four gages were lost while testing - one core OGV and three on the stage one vanes. Due to the planned redundancy in the number of gages at each vane location, there was no detrimental effect on the quality of fan stator monitoring as a result of gage loss.

In the operation of the test vehicle, air entered the plenum ahead of the vehicle through a 4.6 meters (15 feet) diameter, 11.3 meters (37 feet) high, vertical inlet stack. A motor-operated valve located in the top portion of the inlet stack allowed throttling of the fan inlet to simulate low pressure altitude conditions. Turning vanes at the base of the stack turned the incoming air 90° to enter the inlet plenum chamber. This chamber had a screen at its forward end to prevent the admission of any foreign objects into the fan. A screen on the aft end had 24 thermocouples attached to it, measuring the fan vehicle inlet temperature. The plenum chamber was mounted on wheels to permit its movement forward or aft for adjusting to the length of different test vehicles. For the E^3 fan, this plenum chamber was located as far forward of the bellmouth as possible, approximately 1.2 meters (47 inches). The fan test vehicle was located between the inlet plenum and the discharge air collector.

The total fan airflow entered the bellmouth, located 1.25 fan diameters upstream of the fan rotor blade, after exiting the inlet stack and plenum chamber. The bellmouth flow-measurement station (Plane 10), where the inlet total pressure is also measured, was located 0.62 diameters ahead of the fan. The total airflow entered the fan rotor and was split by the quarter-stage island such that 22% of the flow passed through the booster. Downstream of the booster rotor, the flow was split again such that 42% of the booster flow re-entered the bypass stream and the remaining flow entered the transition duct and core flow measuring section.

The air was discharged from the fan vehicle through two motor operated vane-type discharge valves, one for the core flow and one for the fan bypass flow. The bypass discharge valve directed the air into the main air collector which led up through the facility roof and into a vertical exhaust stack. The core discharge valve directed its air into a smaller air collector and exhausted it to the atmosphere through two vertical stacks each containing an

Table I. Fan Stator Vane Strain Gage Locations.

Core OGV

Item	Qty	Location
1	5	Trailing Edge ID Concave
2	2	Trailing Edge ID Convex
3	3	Trailing Edge Pitchline Concave
4	5	Leading Edge OD Conca ve

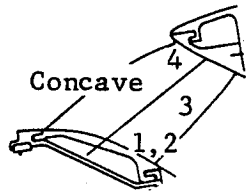

Stage 1 Vane

1	6	Trailing Edge OD Concave
2	3	Trailing Edge ID Convex
3	3	Leading Edge ID Concave
4	3	Hi-C Pitchline Concave

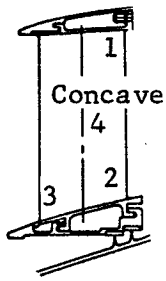

Bypass OGV

1	4	Trailing Edge ID Concave
2	1	Trailing Edge OD Concave
3	2	Trailing Edge ID Convex
4	4	Leading Edge OD Concave
5	4	Tang. to Midspan Island

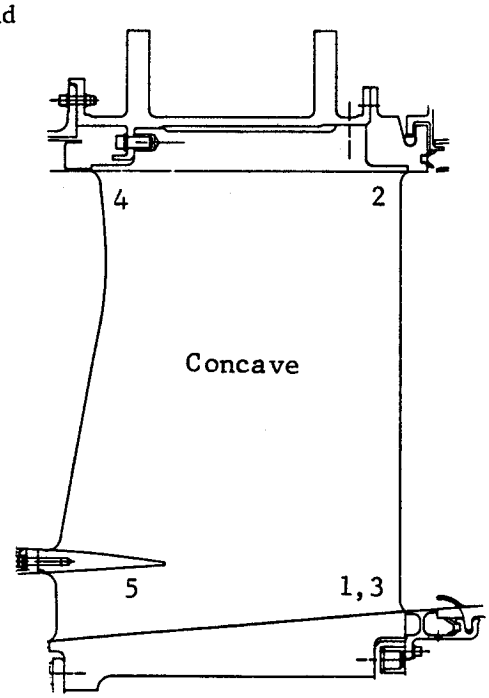

ASME calibrated flow nozzle. The total airflow measurement was determined by the calculation of the bellmouth flow from the measured values of total temperature, total pressure, static pressure, and bellmouth area. The fan bypass flow was the difference between the calculated inlet airflow and the measured core discharge airflow in the two ASME nozzles.

SECTION III

TEST PROCEDURE

The fan component test program consisted of 81.6 hours of testing, divided into three principal phases. The purpose and objective of each phase is described below.

Phase 1 - Mechanical Checkout and Preliminary Performance

The primary purpose of the initial test phase was to verify that the mechanical systems associated with the test vehicle and the test facility were functioning safely and properly. High vibration levels were encountered on the steam turbine drive system during the initial phase of fan testing in September 1981. The steam turbine was repaired and the fan testing was resumed on November 4, 1981.

The fan test vehicle was accelerated to 101.5% of design speed on a low operating line in order to avoid the possibility of encountering stall. The bypass and core discharge valve settings were individually set to approximate the design bypass ratio and data points were taken at 40, 50, 60, 70, 80, 90, 95, 100 and 105 percent corrected speeds. At 90 and 95% speed, the fan was throttled up to points just above the SLS operating line, holding the design bypass ratio constant. Data were also taken along a line approximately at the SLS operating line, from 40 to 90% corrected speed. The performance readings taken during this phase provided the means to check out the instrumentation, data acquisition, and data recording systems.

Phase 2- Performance Mapping

The stall line was determined at the lower speeds, in the 40% to 80% corrected speed range to indicate the severity of stall stresses and to provide early experience with stall recovery procedures and transient operation of the vehicle. Main and core discharge valve positions were established in order to set the design bypass ratio while throttling the fan. In stalling the fan vehicle, the core discharge valve was partially closed before closing the bypass discharge valve to stall. Data points were recorded at 40, 50, 60, 70,

and 80 percent corrected speed, sufficient to establish the required operating line discharge valve settings. Near-stall data points were recorded first by clearing the stalled condition with a wide open discharge valve and second, by throttling back to within a few counts of the bypass discharge valve setting at stall. Operating line data points at 85 to 105% corrected speed were then taken before the high speed stall test.

The fan was intentionally stalled at 85, 90 and 95% corrected speeds to determine the high speed stall line. Stalls at higher speeds were not possible due to the limited available horsepower of the facility steam turbine. The performance map was defined from low operating lines to stall with a minimum of eight data points recorded for each speed line from 40 to 95% speed. At 100% speed, seven data points were recorded from just below the cruise operating line to the point where the flow had rolled back approximately 6% from the operating line flow. Only three points were taken above 100% speed due to the horsepower limitations. All data were recorded with bypass ratios near the nominal design value of 6.8.

Phase 3 - Bypass Ratio Excursion Performance

At both 90% and 95% design speeds, the bypass ratio was set for four separate off-design conditions with bypass ratios larger and smaller than the design value. Stalls were intentionally made with each bypass ratio. Data were recorded near stall and above and below the nominal operating line.

SECTION IV

AERODYNAMIC PERFORMANCE

Clean-inlet performance test data readings were taken at fan speeds ranging from 40% to 105% of the design corrected speed. Several data points were recorded at each speed line from a low operating line to a near-stall point. Stalls were intentionally induced by throttling the fan with closure of the bypass discharge valve at speeds from 40 to 95%. At speeds above 95%, test vehicle operation was limited by the available drive-turbine horsepower, and, stalls and near-stall data points were not possible. Most of the test readings were taken with design or near-design bypass ratios; a separate portion of the test was carried out with off-design bypass ratios at 90 and 95% corrected speeds.

A. Fan Bypass

The fan bypass performance map is shown in Figure 3. The total fan airflow is measured by the pitot-static rakes at the bellmouth throat (Plane 10) and then corrected to the fan face (Plane 12) average conditions by the amount of un-sensed total pressure occurring from wall boundary layer buildup. Momentum-averaged properties are used to calculate adiabatic efficiencies at Plane 14. The momentum-averaging method performs the total-pressure averaging calculation as if all stream tubes were completely mixed at the location of the Plane 14 rakes. In reality the mixing occurs gradually over some distance downstream and will probably not be complete even at the nozzle exit. For this reason, the definition of fan efficiency given here will lead to a slight underestimation of the thrust produced by the engine. The bypass pressure ratio on the fan map is caluclated from the momentum-averaged arc rake total-pressure, adjusted for any circumferential variations at Plane 14, and the fan face average total-pressure. The adiabatic efficiencies shown for each data point are calculated by using the adjusted, momentum-averaged properties at Plane 14 and the fan face (Plane 12) average conditions. A tabulation of all data points shown on the map is presented in Appendix I. The measured flow, pressure ratio, adiabatic efficiency and bypass ratio, as well as the fully-adjusted values, are listed for each data reading.

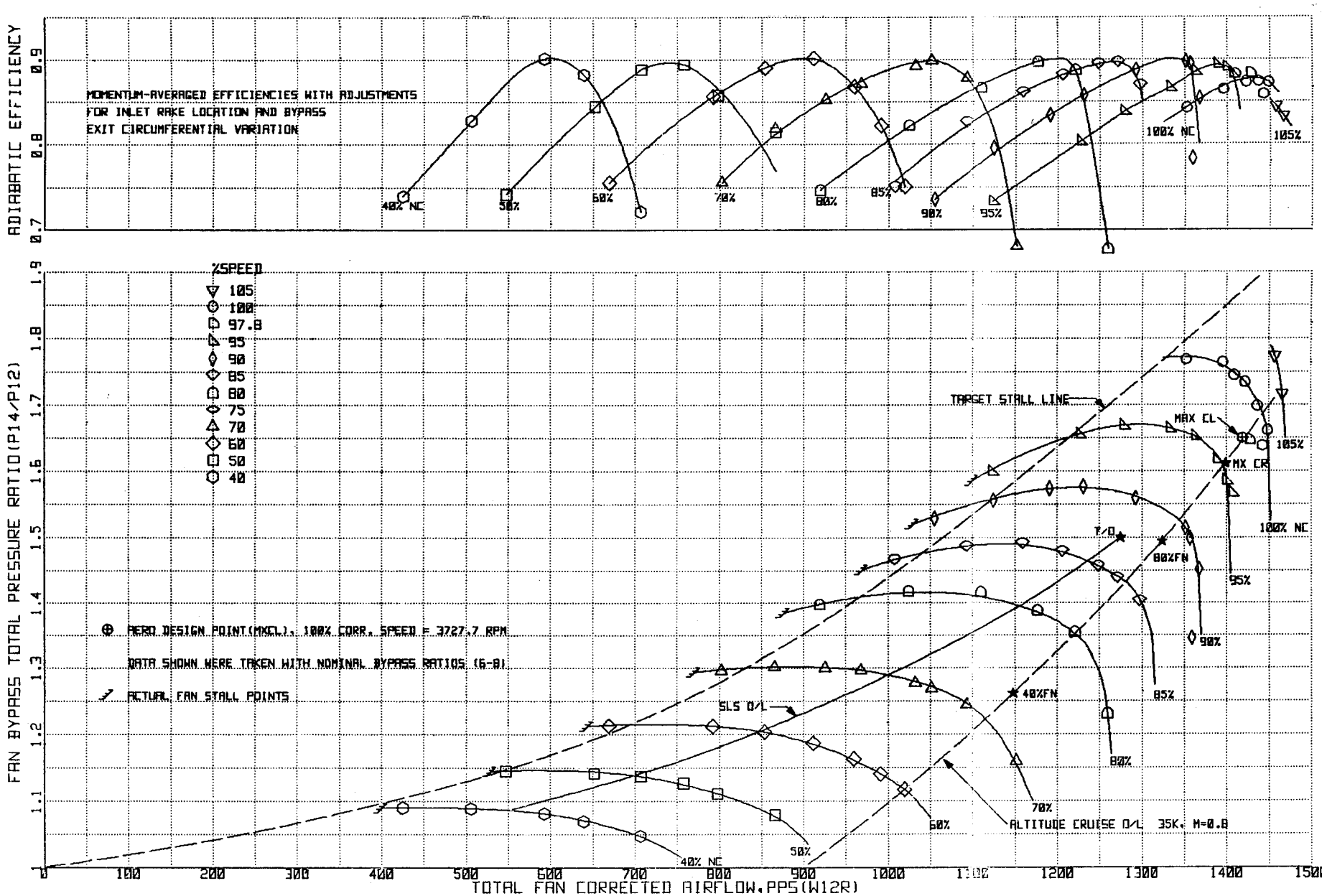

Figure 3. Fan Bypass Component Performance Map.

The measured total airflow was higher than predicted at all speeds by 1.4 to 3.5%. It is believed that approximately 0.5% of the flow is due to a slightly more open flow induction surface in the blade tip region, as deduced from a data match calculation. The rest of the flow is probably due to a better bellmouth flow coefficient than that used in the flow calculation. The design airflow of 643.7 Kg/sec (1419.2 lbm/sec) was reached at 97.5% corrected speed at the design pressure ratio of 1.65. Test-measured stall points were determined for all speed lines up through 95% corrected speed. The target stall line was exceeded by approximately 3.0 to 5.0% at speeds above 50%. The stall margin available at the sea level takeoff condition is approximately 15% at a constant airflow.

The total corrected airflow and bypass pressure ratio were adjusted for the loss in total pressure between Plane 10 and Plane 12 caused by the inlet duct boundary layer, which represents the un-sensed total pressure. This loss amounted to approximately 0.6 point in bypass adiabatic efficiency. The bypass efficiencies were further adjusted to account for momentum averaging and circumferential sampling variations at Plane 14. The resulting momentum-averaged efficiency was approximately one-half point less than the mass-weighted value. The core-stream pressures and efficiencies were the as-measured values since the inlet wall-friction loss and momentum-averaging method did not apply.

The radial profiles of pressure, temperature and adiabatic efficiency were analyzed for reading No. 153 near the maximum climb aerodynamic design point. Figure 4 shows the total pressure ration versus the design stream-function. At the left of the Figure are the boundary layer rake element pressures and the the Plane 10 radial rake pressures ratioed to the average plane 10 total pressure. To the right of the figure are the bypass arc rake, radial rake, and vane-mounted elements. The stator 1 vane-mounted data are also shown. The range of total pressure in the wakes behind the OGV's are shown by the leader lines drawn from the circle symbols. The radial rake data are indicated by the triangular symbols. The rotor part-span shroud, island and core splitter locations are indicated on the figure. The solid (stage exit) and dashed (rotor exit) lines show that the aerodynamic design intent distribution of pressure ratio was achieved.

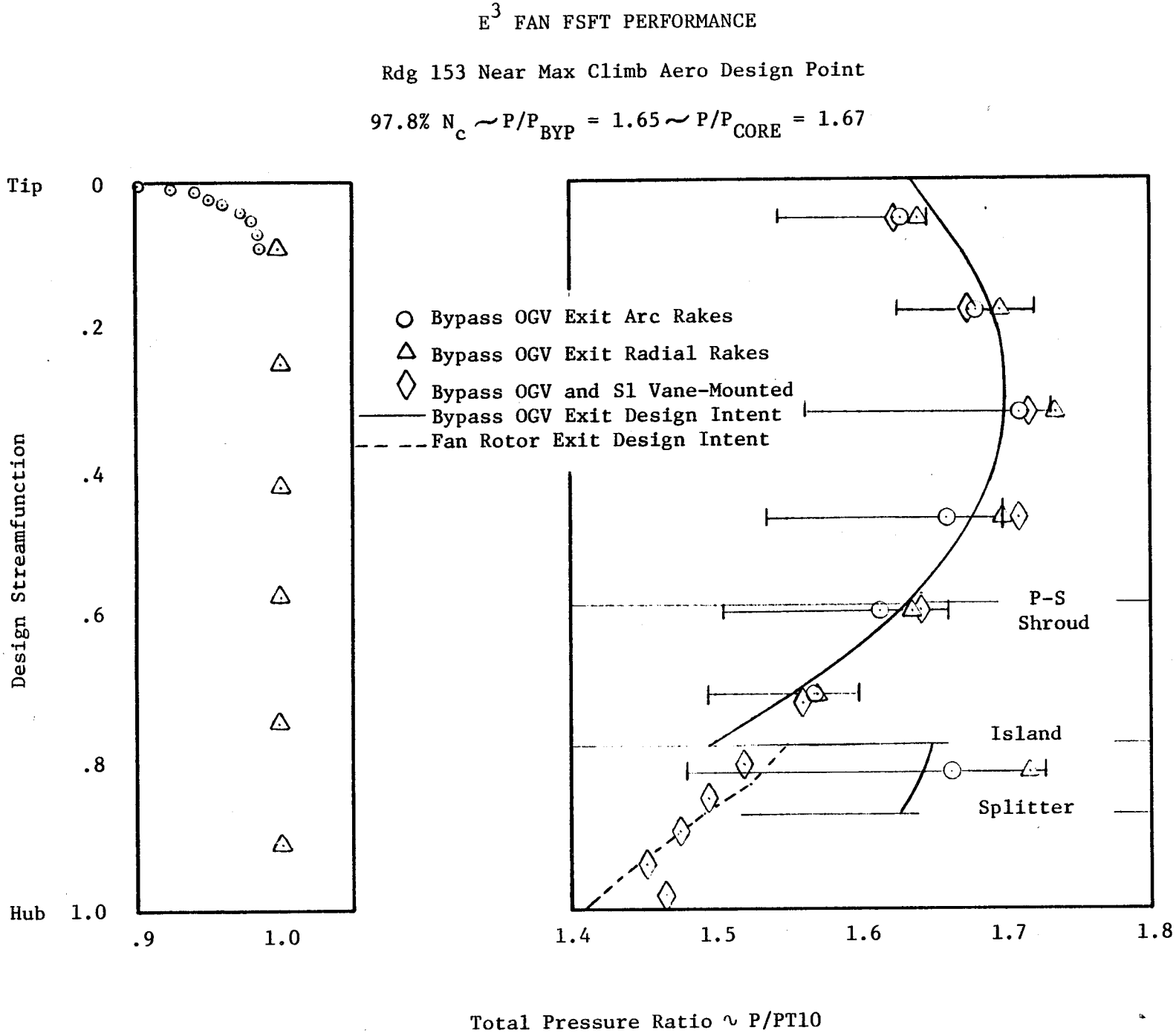

Figure 4. Fan (FSFT) Bypass Performance - Total Pressure Ratio.

The total temperature data and efficiency profiles for the same reading are shown in Figure 5. Again, the design intent profiles were closely matched by the test data. The efficiency profile shows that the fan exceeded the design intent efficiency goal in the tip region and the region just above the island streamline location.

The booster spill flow that passed above the core splitter and mixed with the bypass flow appeared to match the design intent quite well. This flow was calculated from the total and static pressure and total temperature measurements at plane 93 using the design area coefficient. When the two flow streams were throttled to achieve the design bypass ratio of 6.8, the design bypass and core stream pressure ratios of 1.65 and 1.67, respectively, were produced. The amount of spill flow at the maximum climb data point was measured to be 46% of the total booster flow, very nearly equal to the design intent of 43%.

Figures 6, 7 and 8 show arc rake profiles of total pressure, total temperature and adiabatic efficiency at each of the 7 radial immersions behind the bypass OGV. The radial rake elements and leading edge vane-mounted elements associated with each arc rake are also shown, and these closely match the highest values on the arc rake. The 10 elements on each arc rake span one OGV blade pitch with the "E" element located behind the vane trailing edge. The loss in efficiency across the OGV is labeled for each immersion in Figure 8. The tip and hub immersions seem to show the largest OGV wake efficiency loss, with the total OGV loss amounting to approximately 3 points in bypass stream adiabatic efficiency. The bypass stream efficiency measurements were adjusted for circumferential variation due to the non-uniformity of the flow by comparing the radial rake measurements at each arc rake immersion. The amount of total pressure or temperature difference between the highest arc rake value and the radial rake average at that immersion was subtracted from the arc rake average, and for that value a new efficiency was calculated.

B. Fan Hub and Quarter-Stage

The core-stream performance map is shown in Figure 9. The core-stream corrected airflow is the flow that enters the core-flow measuring section downsteam of the frame strut trailing edge (Plane 25), corrected to the fan inlet.

E^3 FAN FSFT PERFORMANCE

Rdg 153 Near Max Climb Aero Design Point

97.8% Corrected Speed

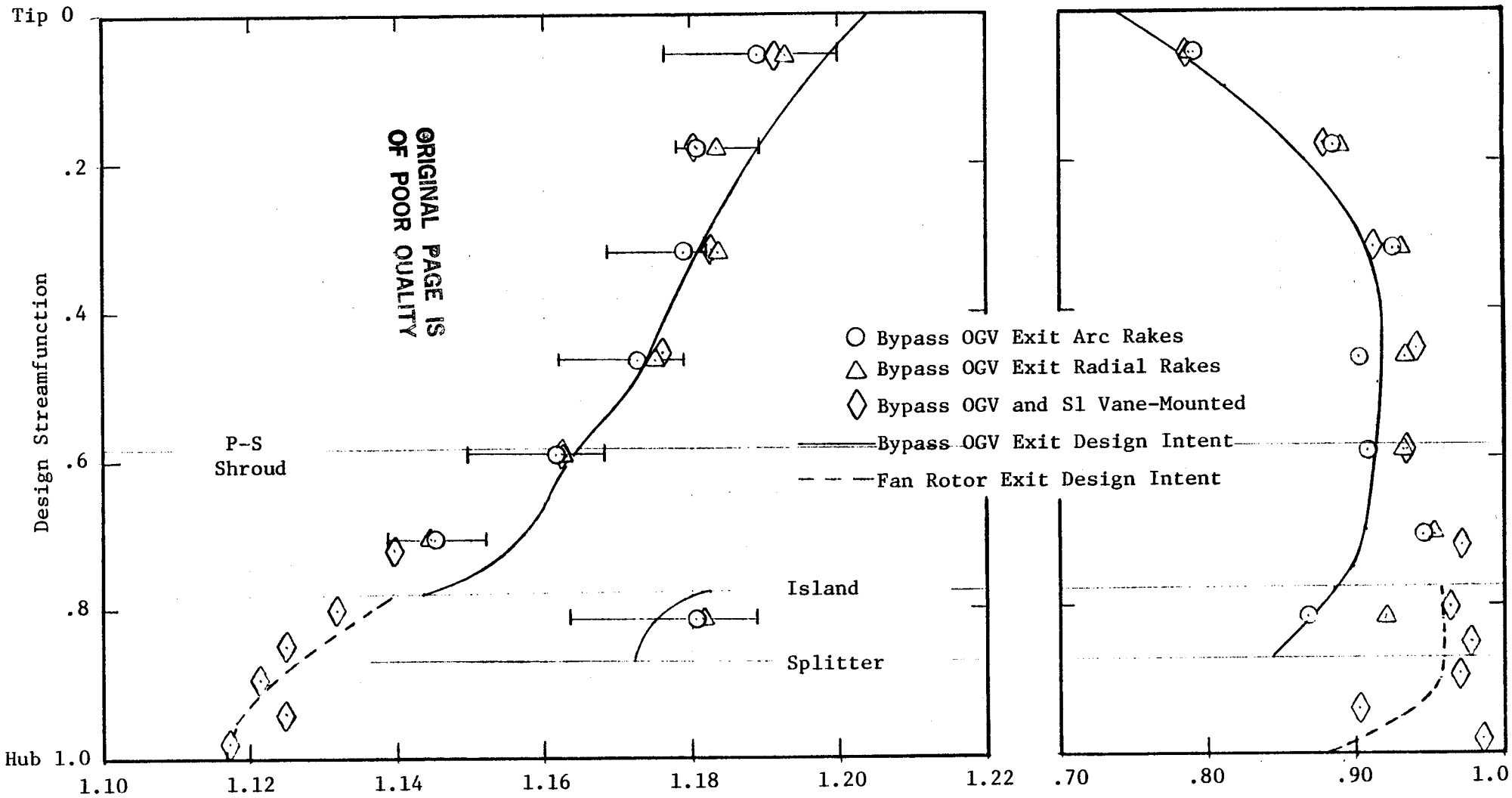

Figure 5. Fan (FSFT) Bypass Performance - Total Temperature Ratio and Adiabatic Efficiency.

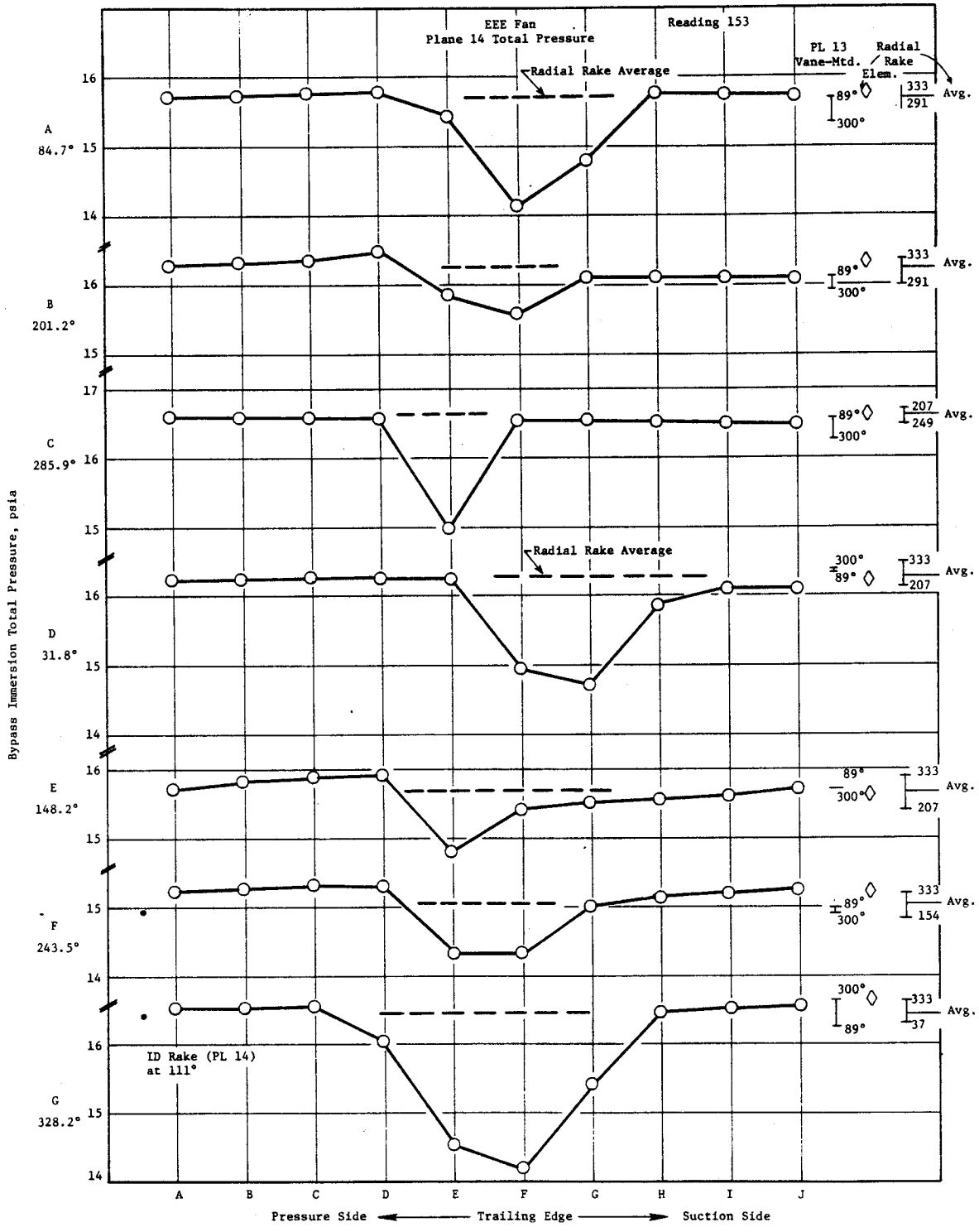

Figure 6. Fan OGV Wake Data - Total Pressure.

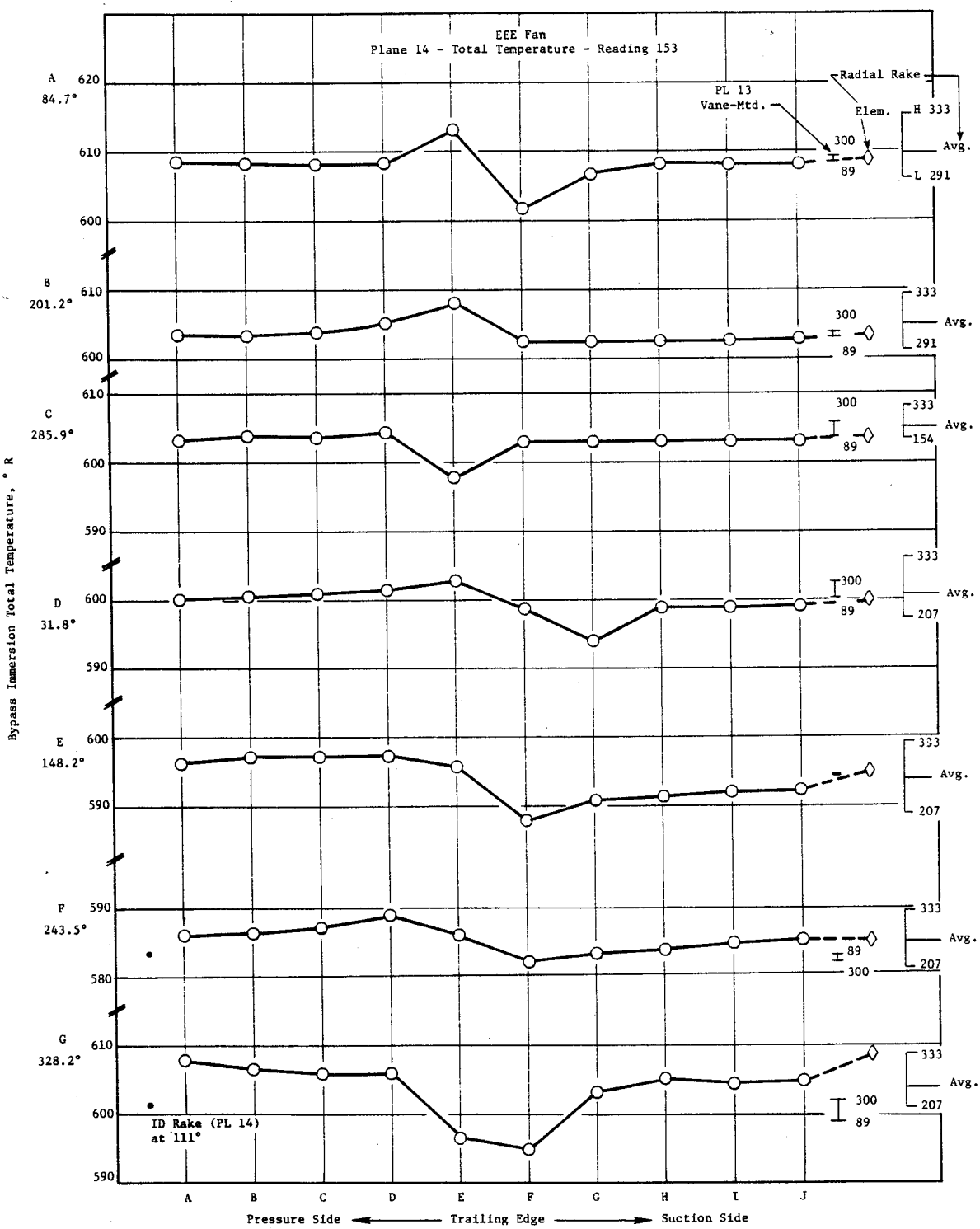

Figure 7. Fan OGV Wake Data - Total Temperature.

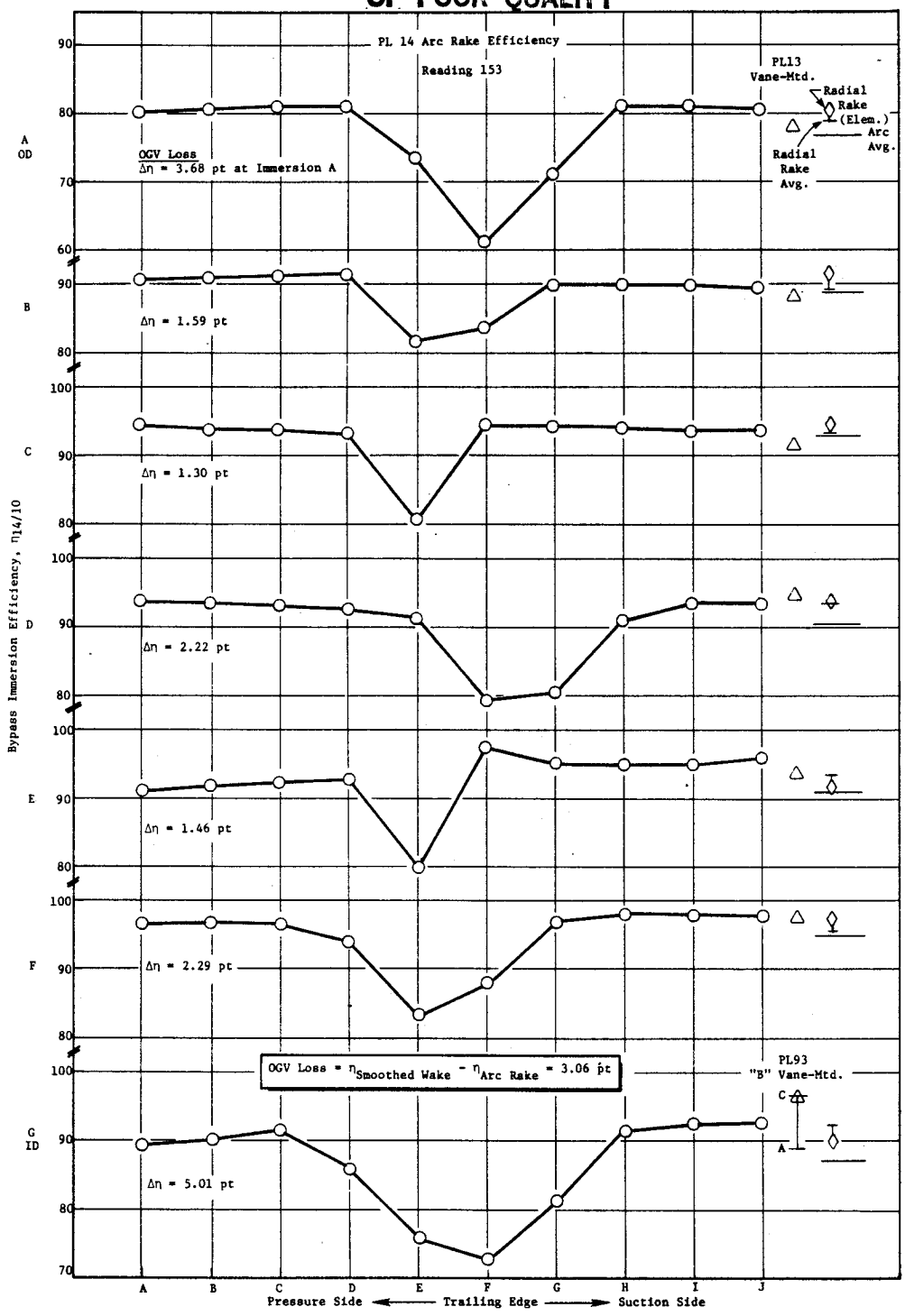

Figure 8. Fan OGV Wake Data - Arc Rake Efficiency.

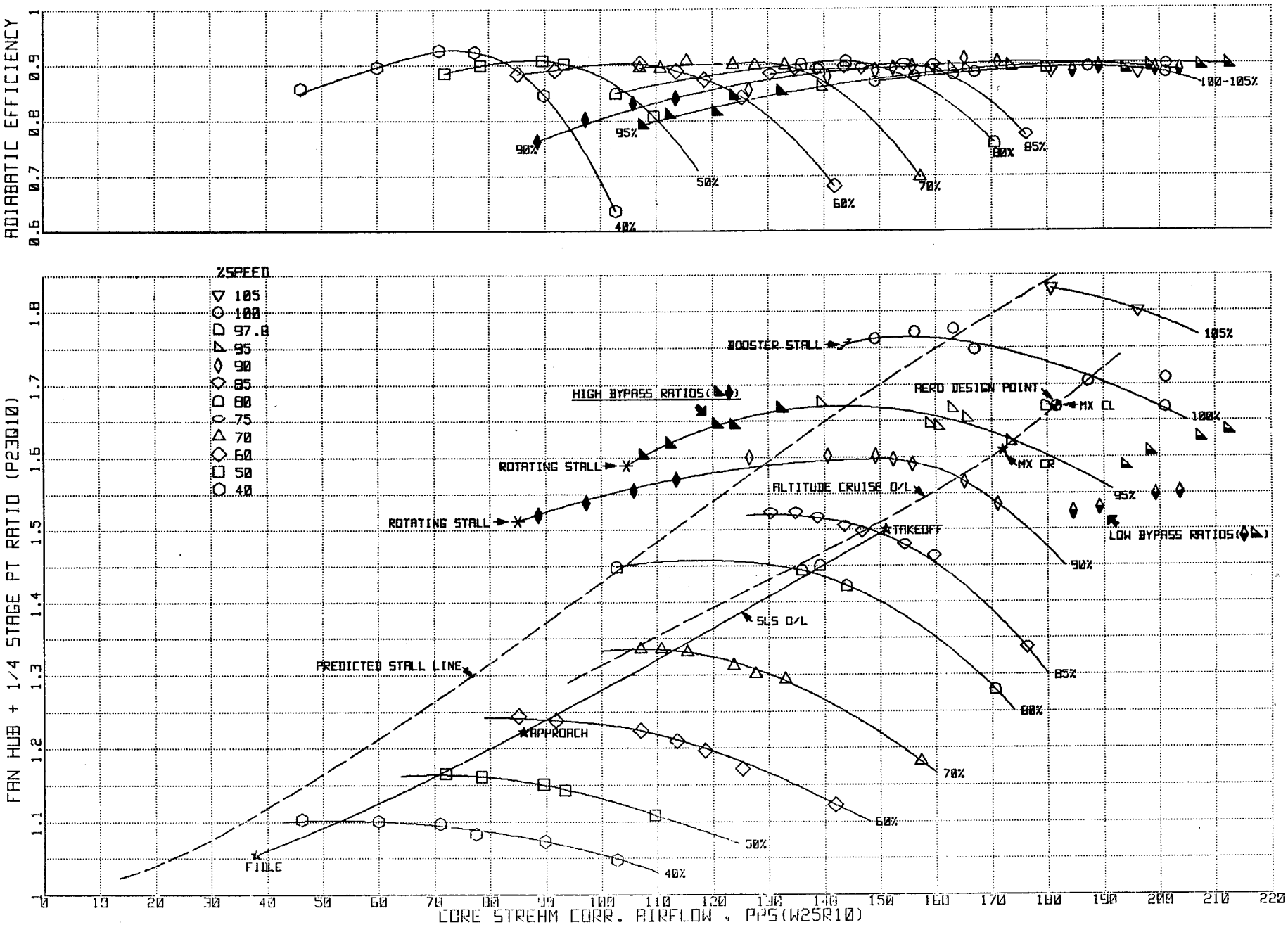

Figure 9. Fan Hub and Quarter-Stage Performance Map.

The pressure ratio is calculated from the inner OGV exit (Plane 23) arc rake mass-averaged total-pressure, ratioed to the Plane 10 inlet total pressure. The seal level static and altitude cruise [M = 0.8, 10.67 km (35000 ft)] operating lines and the predicted stall line are shown. The fully-throttled extremes of the 90 and 95% speed lines are the points of quarter-stage rotating stall. These are approximately 10% in pressure-rise above the predicted stall line and 20-25% margin above the core-stream map operating line. An unintentional full-fan stall occurred at 100% speed when the quarter-stage rotor, operating near-stall, was further throttled to a very high bypass ratio condition. Transient stress survey data showed that the quarter-stage rotor stalled first and back-pressured the fan rotor into a full-fan stall. This point is shown on the 100% speed line approximately 18% above the cruise operating line.

The core-stream total-pressure ratio, total-temperature ratio and adiabatic efficiency profiles for the reading near the max climb aerodynamic design point are shown in Figure 10. The design intent profiles at the OGV exit (solid line) and quarter-stage rotor exit (dashed line) are shown. Relative to design intent, the test data at the OGV exit planes are slightly higher in total-pressure and efficiency at all immersions except the very hub, where the hub boundary layer has weakened the flow. The average efficiency in the core-stream below the splitter has exceeded the design intent by 1.7 points. The diamond-shaped symbols representing the leading-edge vane-mounted data show a very healthy, hub-strong profile entering the core-stream OGV. Exiting the OGV, the profile is weakened in the hub region (inner 2% of total fan flow) and this is carried on through the core frame struts to the compressor inlet station (Plane 25).

C. Bypass Ratio Excursions

The bypass excursion test points are shown on the core-stream performance map (Figure 9) by the shaded symbols at 90 and 95% speeds. The high bypass ratios (7-15) occurred when the core discharge valve was well-closed relative to the nominal position. These data points appear well-above the predicted stall line on the core-stream map. The low bypass ratios (4-6) occurred when the core discharge valve was wide open and the bypass valve was closed. These

Reading 153 Near Maximum Climb Aero Design Point

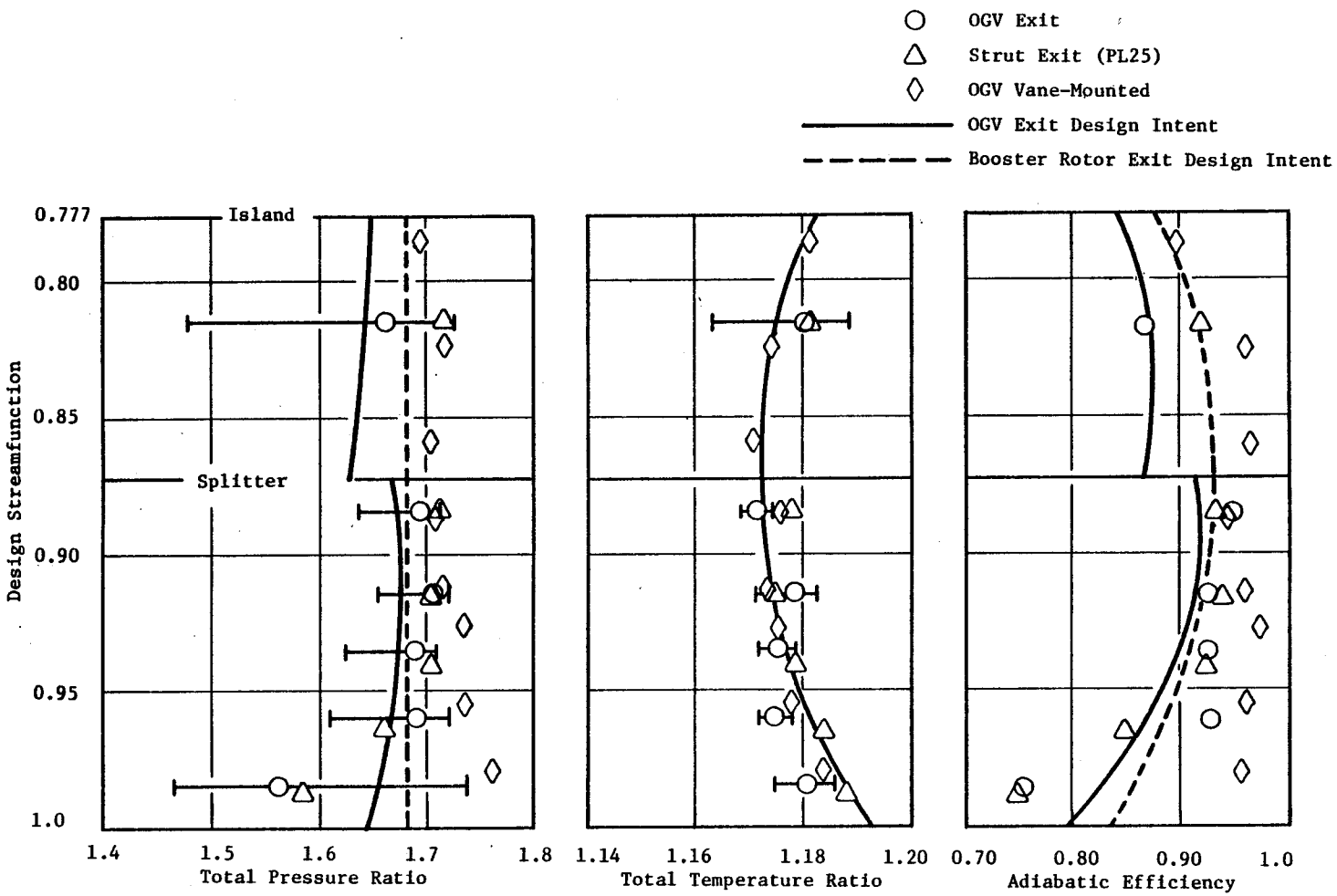

Figure 10. Fan Hub and Quarter-Stage Profiles Near Aero Design Point.

data plot quite low on the map speed lines at 90 and 95% speeds and suggest that the speed-core flow relationship is a function of the bypass ratio; lower bypass ratios produced more core-flow at a given speed. Correspondingly, the high bypass ratios reduced the amount of core flow at speed.

The bypass discharge valve was set at the nominal fan operating line position when the core discharge valve was closed to produce bypass ratios as high as 15:1. When the core valve was closed, the quarter-stage rotor was throttled along a constant, nearly-flat speed line as shown in Figure 9; the bypass stream conditions migrated only slightly from its nominal operating point on the map. At bypass ratios greater than 13:1, the quarter-stage rotor encountered a rotating stall. Further throttling was possible as a full fan stall did not occur, but the rotating stall produced a loud, whining fan noise audible in the test cell area. The stresses on rotor 2 however, remained at a low and safe level. Lower-than-design bypass ratios were achieved by throttling the bypass flow toward stall while the core valve was wide open.

The effect of bypass ratio excursions on the fan bypass-stream performance at 90% speed on the operating line is shown in Figure 11. The OGV exit (Plane 14) adiabatic efficiency, at each of the seven arc rake immersions, is plotted versus bypass ratio. The change in average plane 14 efficiency from the near-nominal bypass ratio point ($\beta = 6.25$) for each increasing bypass ratio is shown at the top of the plot. The drop-off in overall performance is gradual and nearly linear and shows that the best efficiency is achieved near the design bypass ratio. Only the hub immersion, which measures the spill flow performance, drops off rapidly beyond a bypass ratio of 8. The corresponding core-stream efficiencies at each of the five arc rake immersions are shown in Figure 12. The immersion efficiency bypass ratios above 8:1 are steeper than the bypass immersions show, except at the hub where the efficiency was not very high even at the design bypass ratio. The change in average plane 23 efficiency shows a large loss (over 8 points) for the real high bypass ratio.

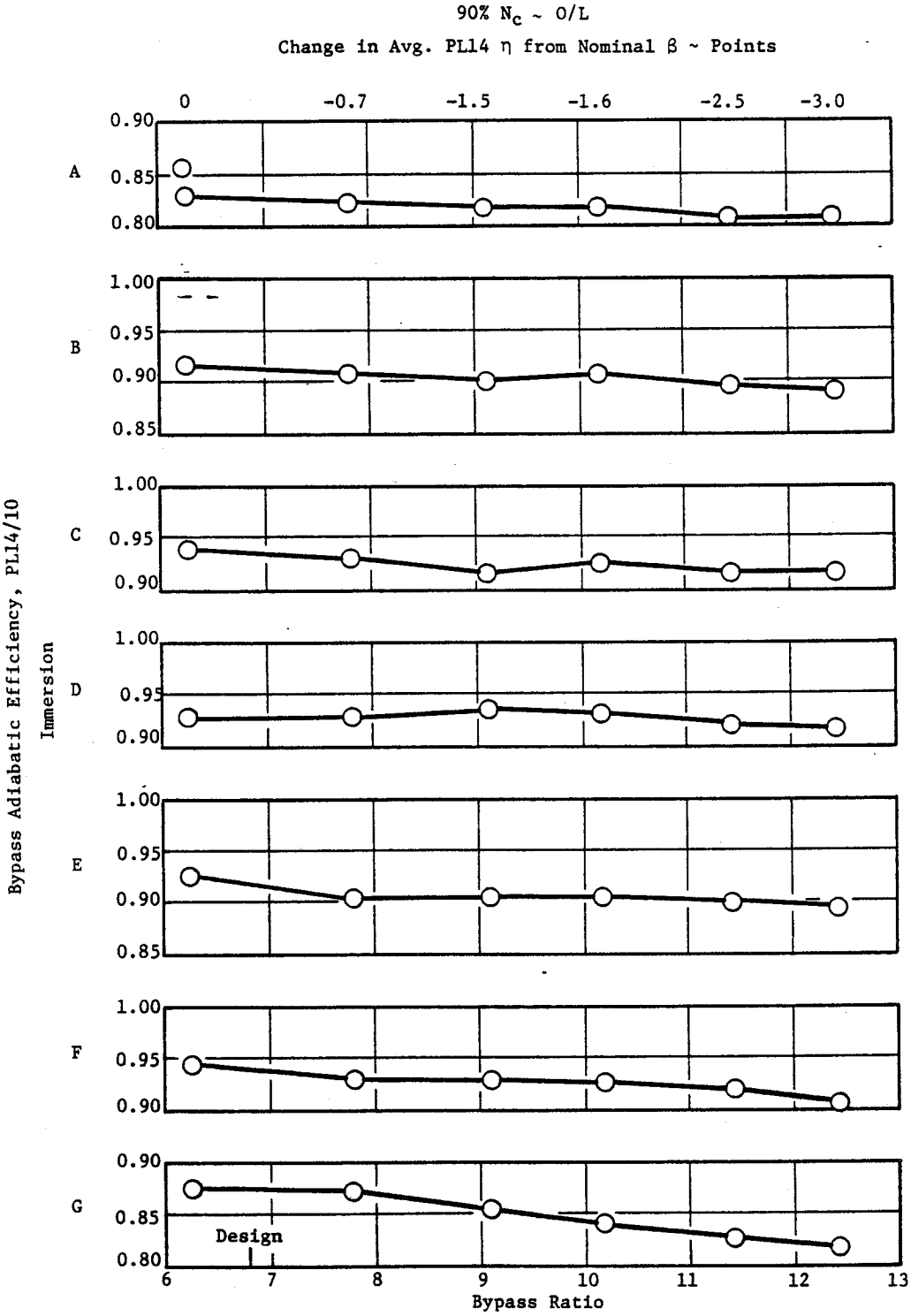

Figure 11. Fan Bypass Efficiency Versus Bypass Ratio at 90% Speed.

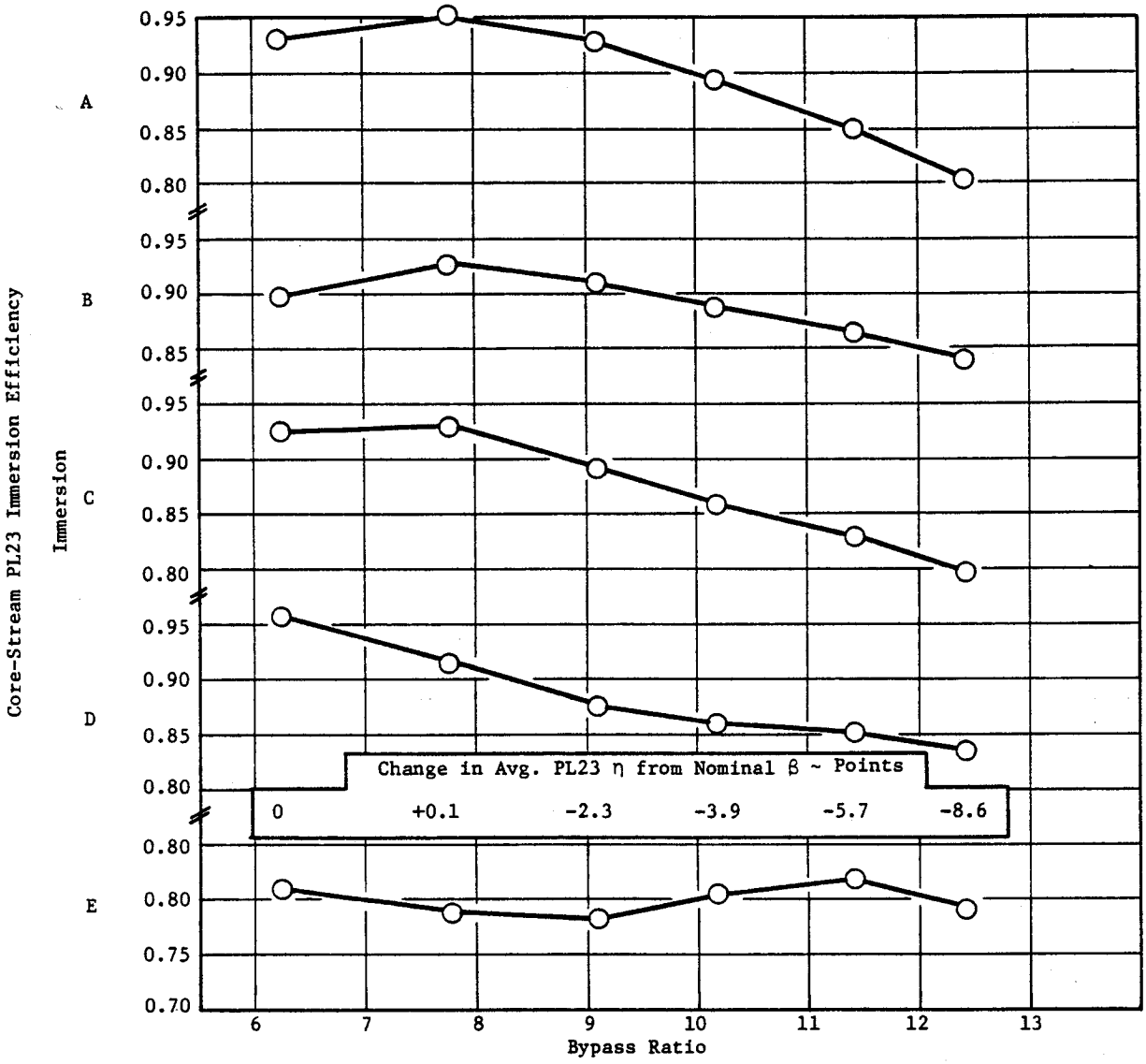

Figure 12. Core Stream Efficiency Versus Bypass Ratio at 90% Speed.

SECTION V

AERO- MECHANICAL PERFORMANCE

A. Fan Rotor

The E^3 fan completed a successful test program of 81.6 hours, including a thorough mechanical checkout, aerodynamic performance mapping and fan stalls.

A maximum speed of 3930 rpm (105.4% physical) was reached and 12 intentional and 2 unintentional stalls were sustained. Normal fan operation produced a maximum fan blade (R1) response of 21 percent of limits and a maximum quarter-stage (R2) response of only 17 percent of limits. The highest stress levels were seen during an unintentional stall at 100 percent speed when 50 percent of limits for R1 and 65 percent of limits for R2 were reached.

The mechanical design goals established for the fan rotor included improved durability, ruggedness, and reduced maintenance. Some of the most important features of the rotor design which give it excellent mechanical reliability are: 15% vibratory margin over 2/rev at maximum speed, improved rotor stiffness and stronger blade attachments, low dovetail stresses, and an anti-clank system to prevent dovetail wear. The design which has a modular disassembly feature, also carries improved torque-transmitting capability of the disk/shaft bolted joint and reduced rotor overhang to minimize unbalance. Additionally, the fan blade is designed to provide good bird-strike resistance. The materials selected for the fan rotor configuration are listed in Table II.

Table II. Fan Rotor List of Materials.

Fan Blades	Titanium 6Al-4V
Fan Disk	Titanium 6Al-4V
Spinner	7075 Aluminum
Spinner Cover	7075 Aluminum
Anticlank Spring	Titanium 6Al-4V
Blade Retention Key	Inco 718
Booster Spool	Titanium 6Al-4V
Booster Blade	Titanium 6Al-4V
Fan Shaft 5/8-inch Bolts	Inco 718
Forward Fan Shaft	4340 Stainless Steel

The fan rotor blade response during normal operation was very well-behaved. The Stage 1 blade 1F mode 3/rev crossing at 2150 rpm produced only a 16 percent of limits response. The first and second system modes were seen but were at levels below 25 percent of limits. At a near-stall condition at 70 percent speed (2610 rpm), the second system mode responded at 25 percent of limits, but diminished to less than 10 percent when the fan was returned toward the operating line. The 2-stripe mode was seen at the 12/rev crossing (3720 rpm) but only responded at 6 percent of limits.

The quarter-stage rotor blades were equally well-behaved. The stage's maximum response occurred at 90 percent speed (3350 rm) when the blade 1F mode reacted with a 5/rev crossing to produce a 17 percent of limits response. The 2 stripe mode responds to a crossing with 120/rev (2 times S1) at 2800 rpm to 16 percent of limits. One hundred and eighty per rev (3 times S1) at 3370 rpm excites a complex mode at 10,080 HZ to 11 percent of limits. During the bypass ratio migration testing at 90 and 95 percent speeds, the quarter-stage rotor blade experienced separated flow vibration at 28 percent of limits. At these test points, the bypass ratio was in the 14.0-16.0 range and the fan was producing a growl that was audible in the control room. Throughout the bypass ratio excursions, the fan blade remained unresponsive to the large bypass ratio swinges.

Intentional stall testing was conducted at 40, 50, 60, 70, 80, 85, 90, and 95 percent speed points. Two additional stalls at each of the 90 and 95 percent speed points were obtained at different bypass ratios. The highest response to these stalls were 48 percent of limits for the fan rotor and 44 percent for the quarter-stage rotor, both in the first flex.

Two unintentional stalls were also encountered. One, at 100 percent speed, happened with the bypass discharge valve fully opened. It was initiated when the main discharge valve was being closed to the 75 percent position causing a much higher than design bypass ratio. Four separate pulses, initiated in the quarter-stage rotor, were sustained before it could be cleared. Since the bypass discharge valve was full open, the stall had to be cleared by opening the inlet valve, and dropping speed. The total stall event lasted 4.25 seconds

and resulted in the fan rotor blade responding to 50 percent of limits (1F) and the quarter-stage rotor blade to 65 percent of limits (1F). The other unintentional stall occurred after taking a steady state reading at 90 percent (Nf) fan speed, at a near-stall condition. When the bypass valve was moved, ostensively toward the open position, a single pulse stall occurred that was cleared by slewing the bypass discharge valve open. Blade instability was not encountered at any condition during the test. At all speeds and bypass ratios, a stall was encountered before any instability was detected.

Figures 13 through 15 show the pre-test predicted Campbell diagrams for the fan rotor and quarter-stage rotor blades. Figures 16 through 19 are Campbell diagrams generated by Fast Fourier Transform (FFT) analysis of strain gage signals from both rotor stages. Figure 16 shows the response of a fan rotor strain gage sensitive to the lower frequency modes while Figure 17 shows a strain gage sensitive to the higher frequencies. Figures 18 and 19 show the similar data for the quarter-stage rotor blades. Figure 20 shows a stability plot of the Reduced Velocity Parameter versus Incidence Angle for the fan rotor blade at various points during the testing. Although the near-stall data points appear close to the predicted flexural and torsional boundaries, no signs of instability were evident. Table III shows the stress levels and operating conditions of all the stall events incurred during the testing.

B. Fan Stator

The fan stator configuration used for the full-scale fan test is shown in Figure 21. The solid 17-4 PH steel bypass OGV's and core struts are non-flight-type designs but the Stator 1 and core OGV vane assemblies are representative of flight-type hardware. Light-weight 7075 aluminum core OGV's and 6061 aluminum inner and outer shrouds were used. In the Stator 1 assembly, the flow splitter casing was aluminum with the Stage 1 vanes being 410 stainless steel. The inner and outer fairings are fabricated from steel for the best Foreign Object Damage (FOD) protection during development tests.

The stage one vanes were well-behaved during the fan component test. Their major response area was a first torsion mode and 32/rev crossing at

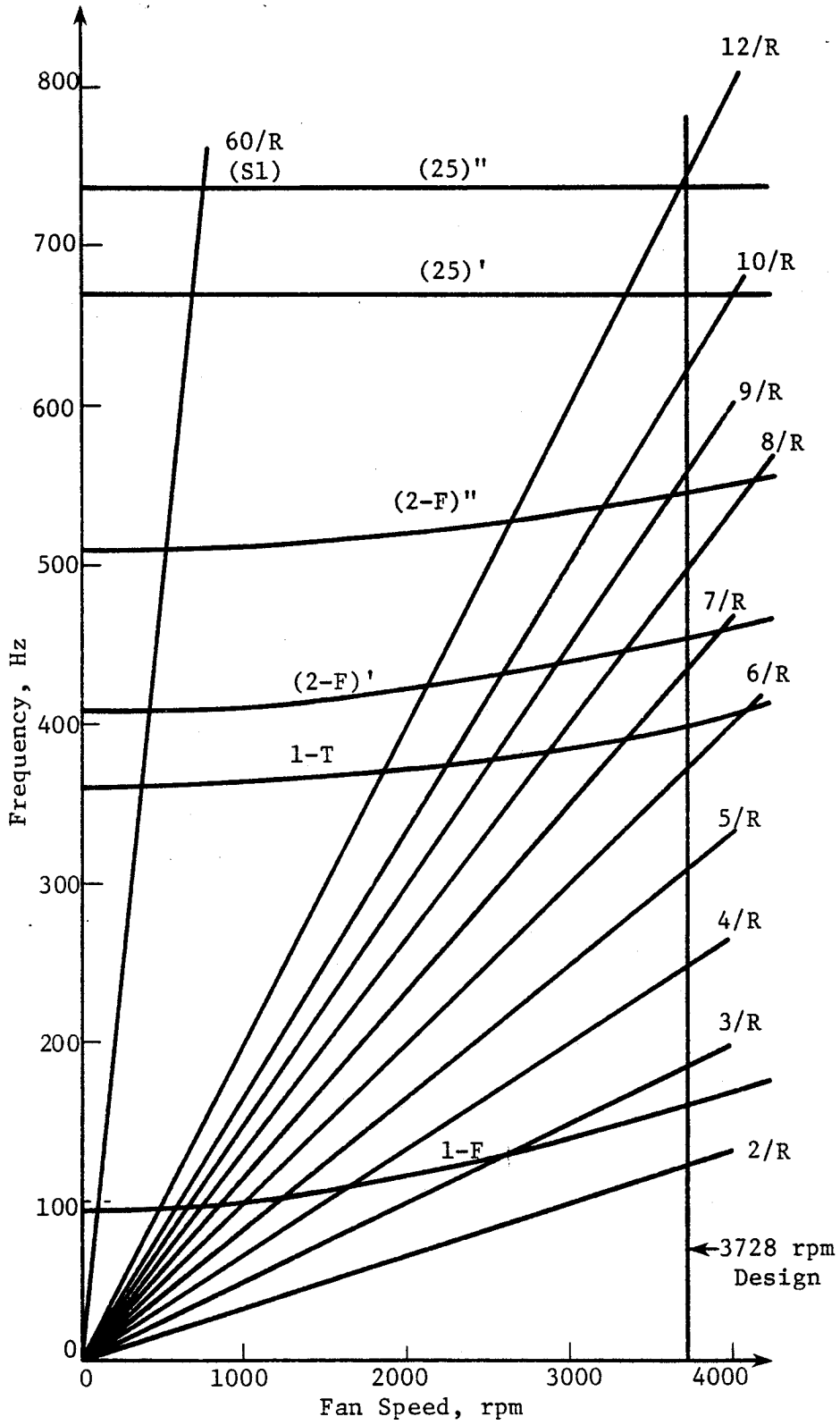

Figure 13. Stage 1 Fan Blade Campbell Diagram (Blade Modes).

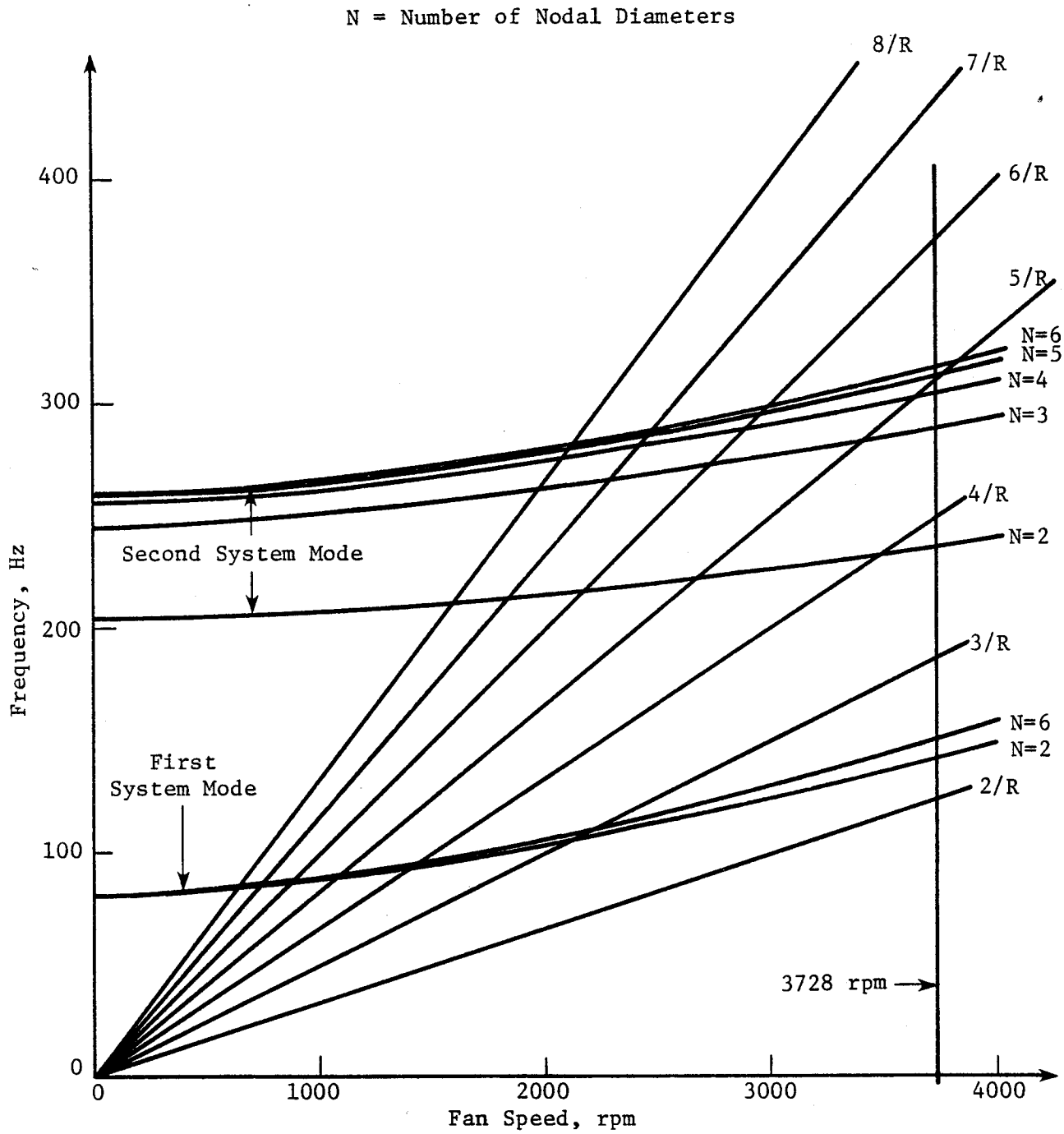

Figure 14. Stage 1 Fan Blade Campbell Diagram (Blade-Disk System Modes).

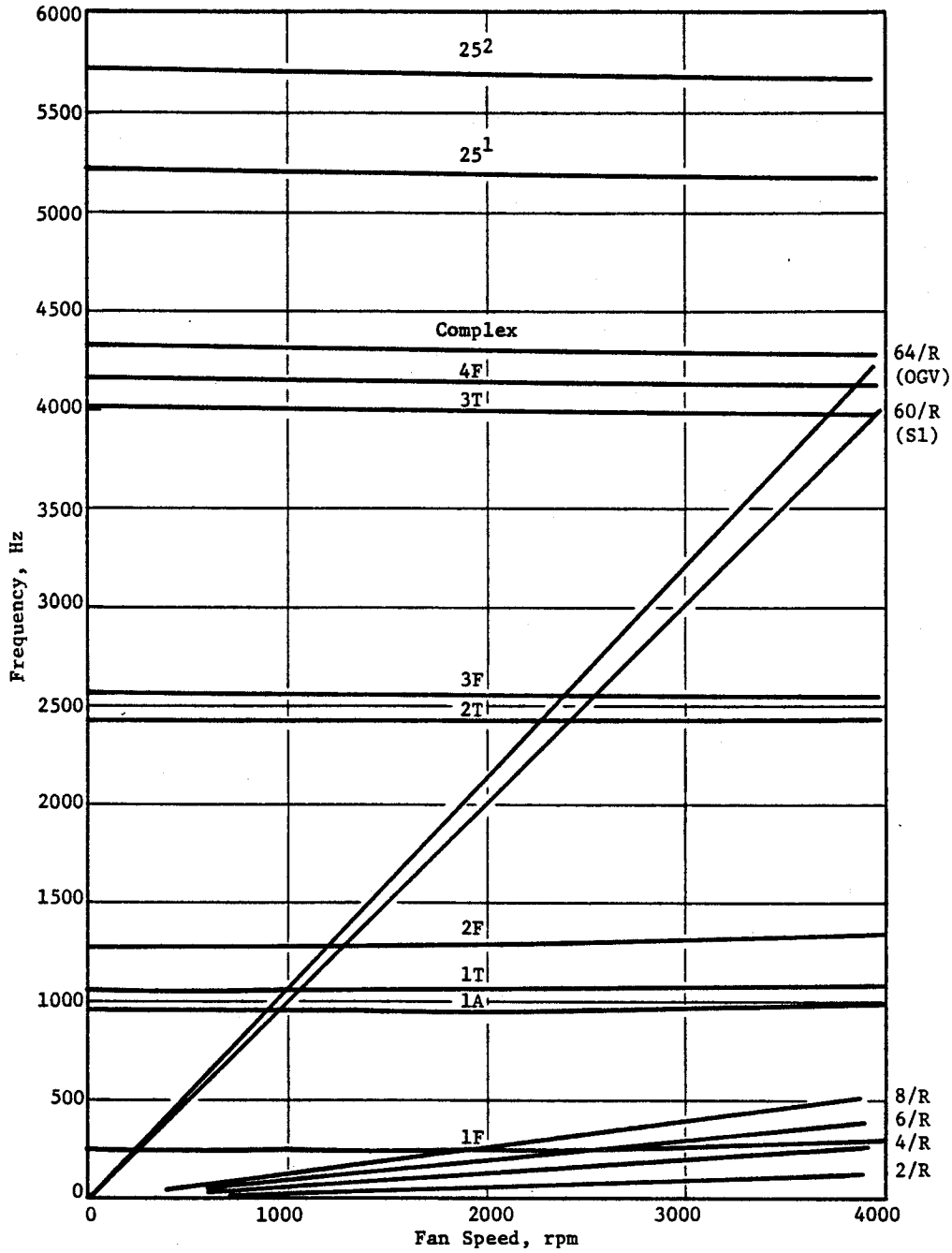

Figure 15. Stage 2 (Quarter-Stage) Blade Campbell Diagram.

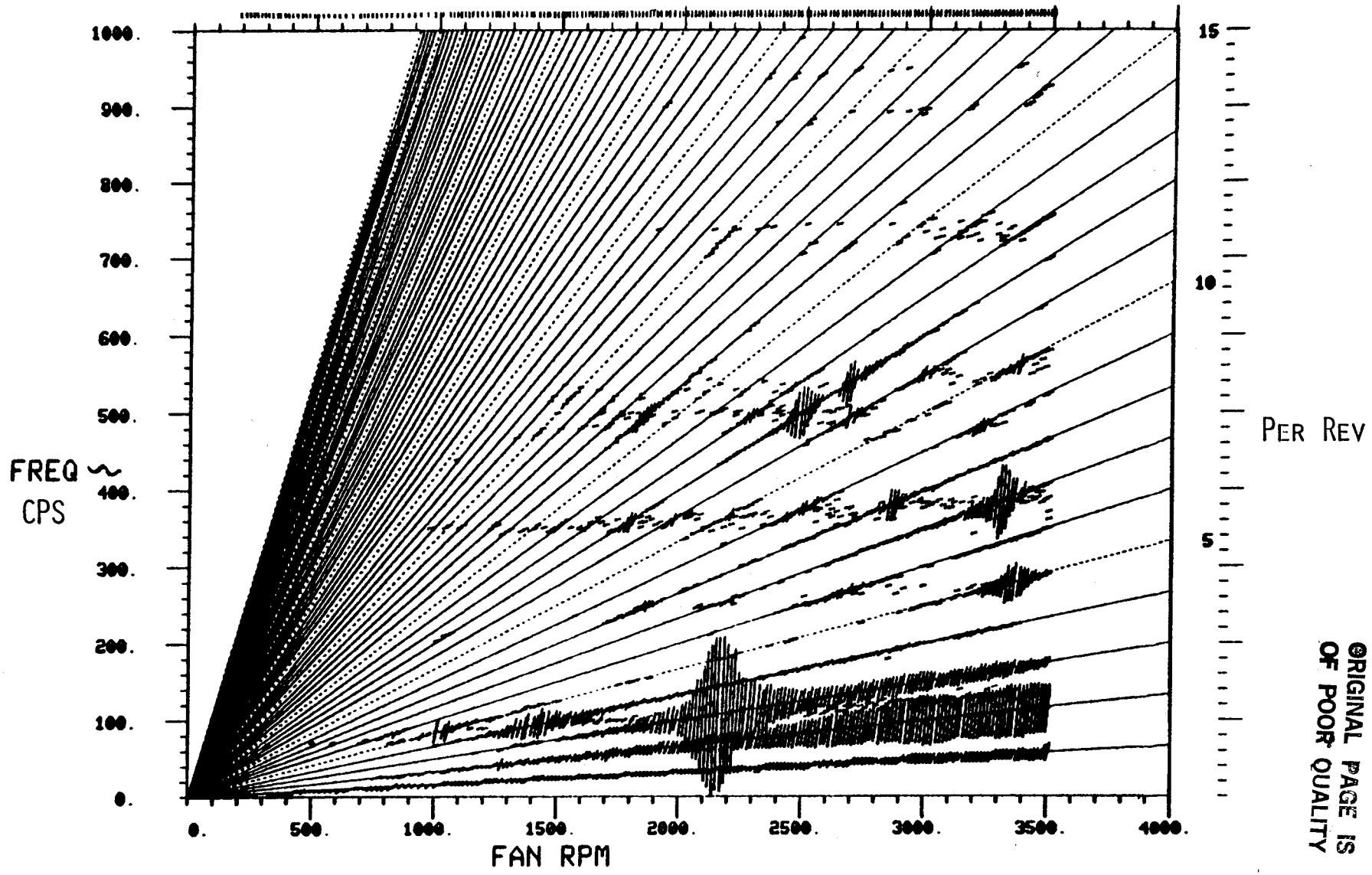

Figure 16. Fan Rotor Low Frequency Response.

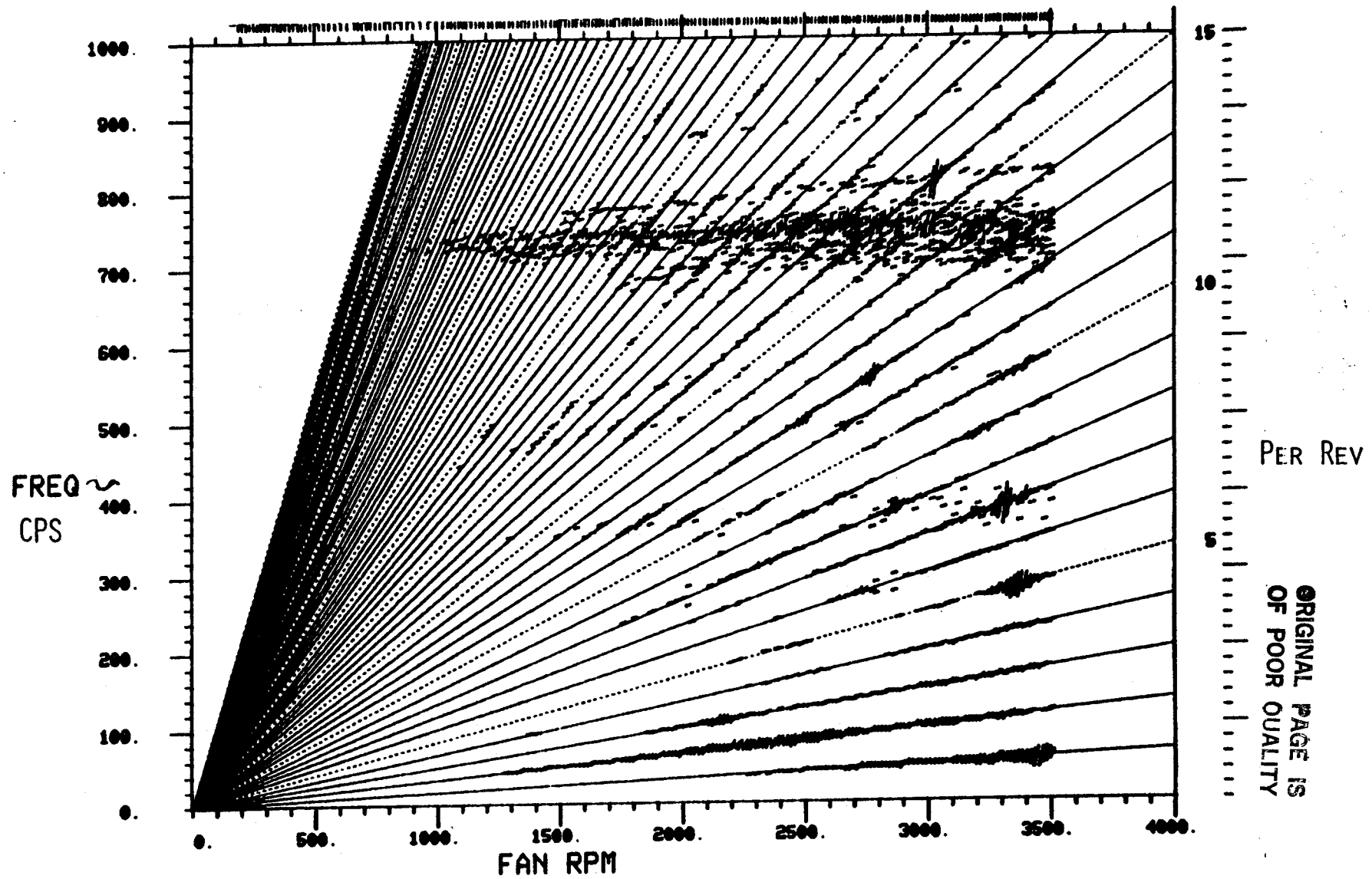

Figure 17. Fan Rotor High Frequency Response.

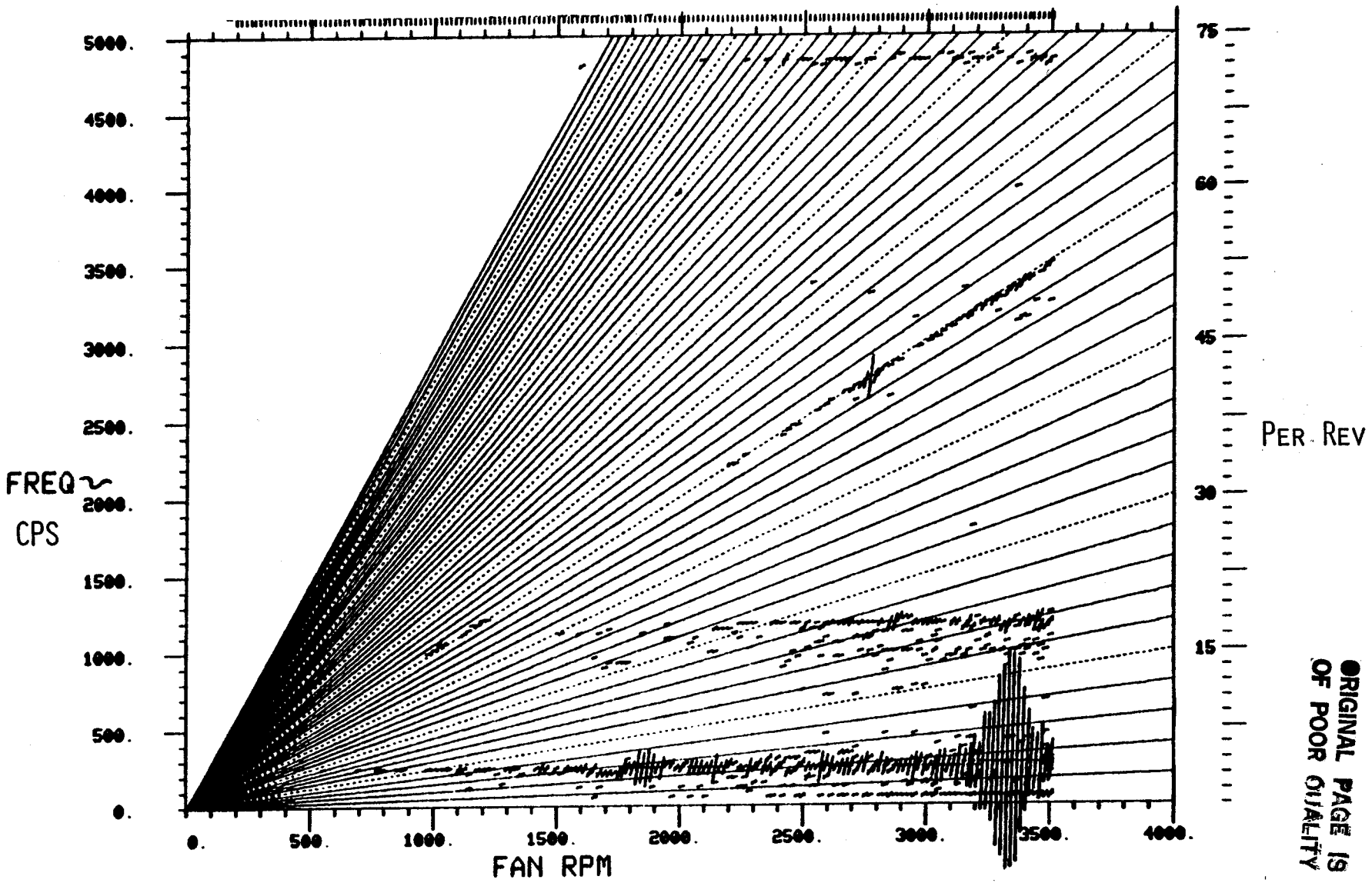

Figure 18. Quarter-Stage Rotor Low Frequency Response.

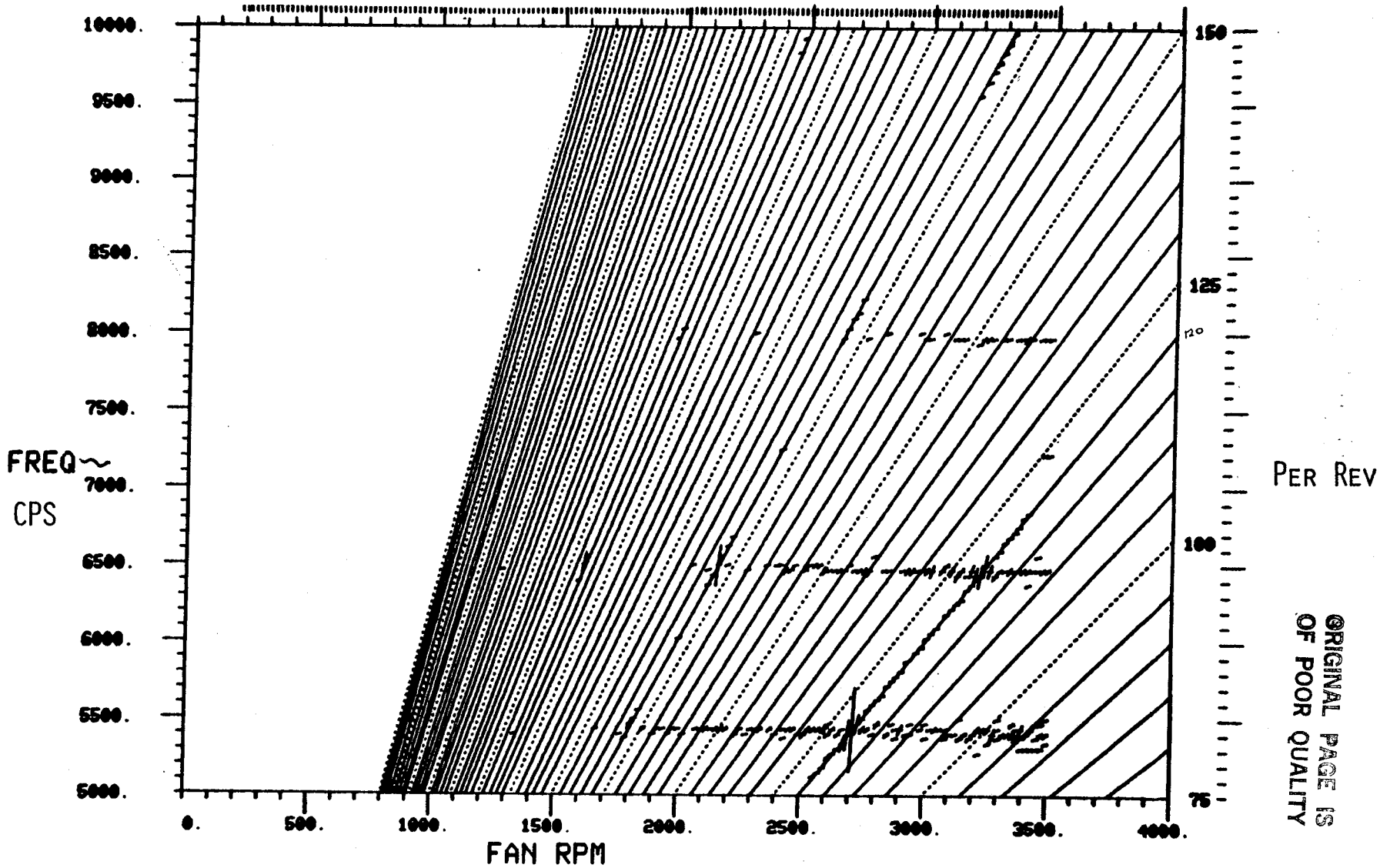

Figure 19. Quarter - Stage Rotor High Frequency Response.

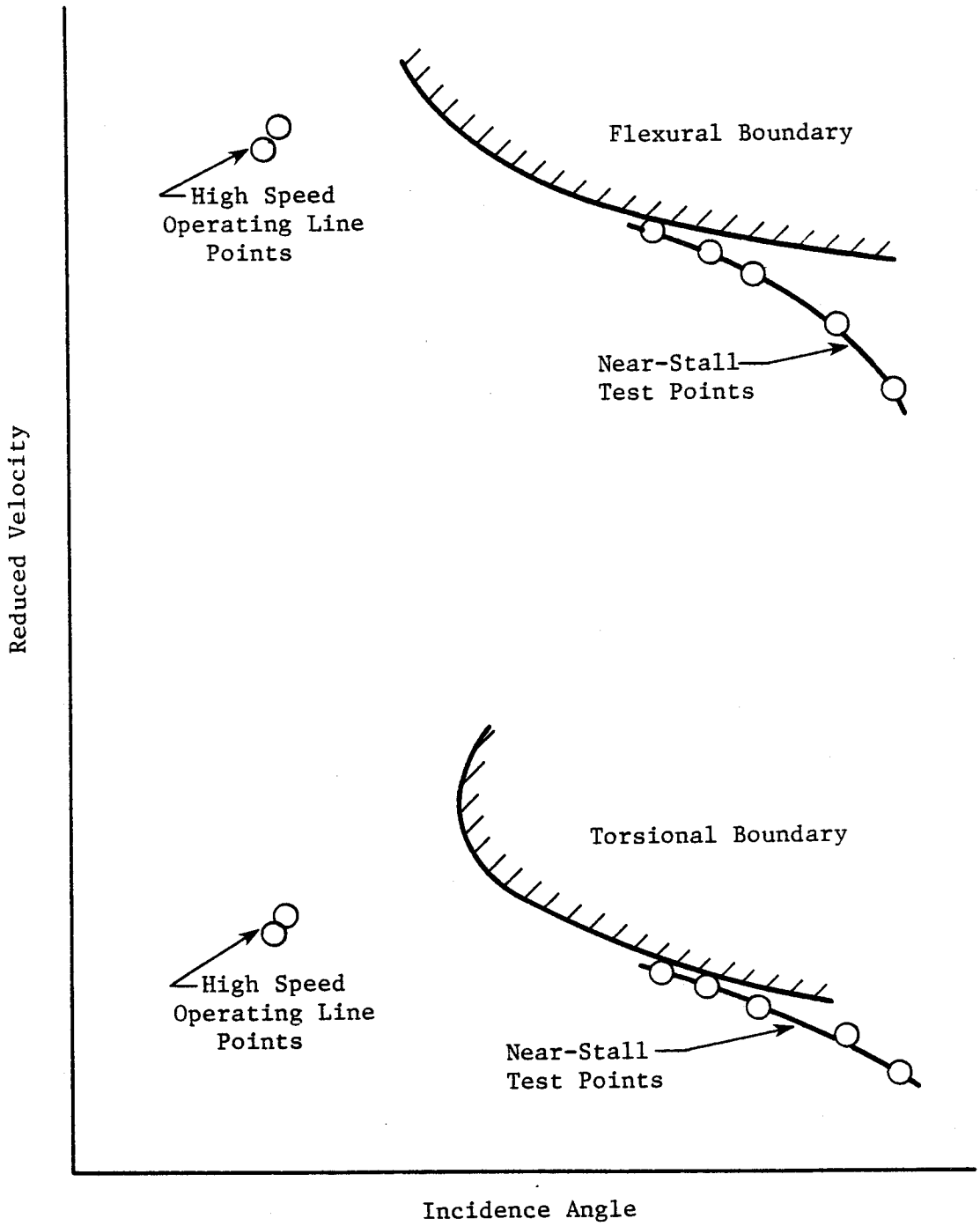

Figure 20. Stage 1 Fan Blade Stability Plot.

Table III. FSFT Blade Stall Events.

% N_f	Physical Speed RPM	Main DV % Position	Bypass DV % Position	Blade Response % Limits	
				Fan Rotor	Quarter-Stage Rotor
40	1481	40	17.0	18	8
50+	1854	50	17.6	---	---
60	2219	50	18.8	38	12
70	2612	60	24.8	38	16
80	2968	50	25.2	40	26
85+	3178	64	28.3	---	---
90	3345	75	29.2	43	33
90	3360	100	29.0	38	31
90	3360	56	29.7	48	41
90*+	3360	56	31	---	---
95	3550	70	31.2	38	44
95	3535	60	30.0	43	41
95	3535	100	32.7	40	28
100*	3732	75.4	100	50	65

*Inadvertent Stalls
+Blade stress levels at these points were not reduced.

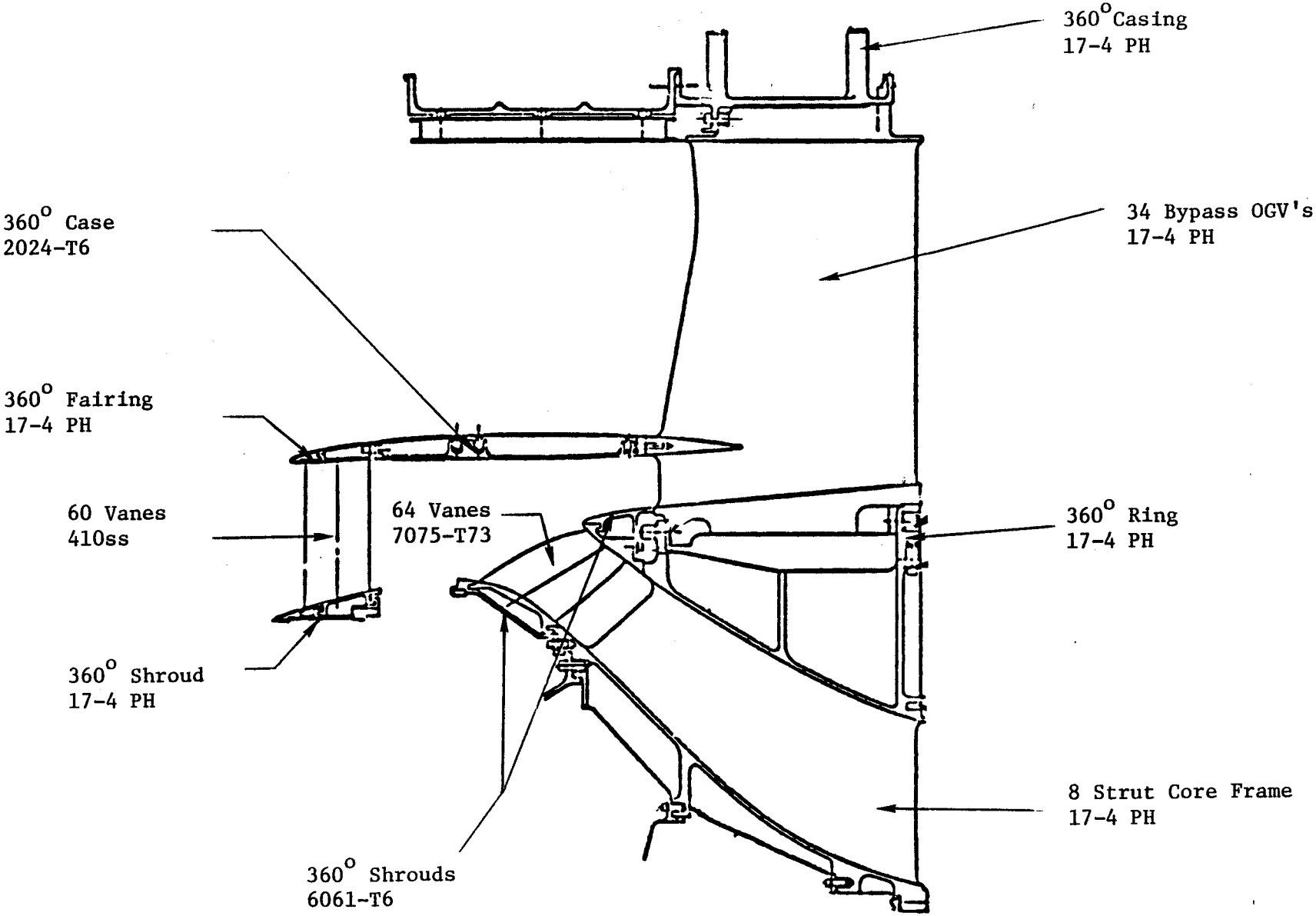

Figure 21. E^3 Fan Stator Configuration.

2600 rpm (70% N_f). The maximum percent of limits seen was 45%. An interaction between first flex mode and 32/rev was observed at 1500 rpm (40% N_f) with a response of less than 20% of limits. The only other mode observed during the testing was a 64/rev and second torsion crossing at 2700 rpm which produced less than 5% of limits. Representative Stage 1 vane Campbell diagrams, generated from fan test data, are presented in Figures 22 and 23. Figure 24 presents a Campbell diagram prepared from analysis and bench testing.

The core OGVs exhibited very little response up to 3500 rpm (94% N_f). However, between 3500 and 3700 rpm, this stage went into a strong resonance due to a 32/rev excitation. The maximum percent of limits was 77% at 3732 rpm (100% N_f). This is the crossing point of 32/rev stimulus and the first torsion mode. The stress levels were the highest during the bypass ratio excursion segments of the test, when the bypass ratio exceeded 13. Since a physical fan speed versus ambient temperature curve for ICLS sea-level-static takeoff conditions shows a maximum fan speed of 3400 rpm, first torsion resonance should not be a problem during ICLS testing. One additional but very minor crossing was stimulated at 2000 rpm (54% N_f) when a 56/rev excited a first torsion mode. Observed limits were well below 10%. Figures 25 and 26 present Campbell diagrams prepared from test data; Figure 27 was generated from bench and analytical data.

Very little response was observed from the bypass vanes at any fan speed. The majority of the strain gage signal was composed of a near 1/rev excitation probably due to a facility disturbance. The fan test data Campbell diagram's are presented in Figures 28 and 29. Note, the very low threshold levels needed to obtain the plot. The Campbell diagram of Figure 30 is the result of bench tests and analysis.

The operating conditions for all of the stall events are presented in Table IV. Physical fan speed, percent corrected speed, bypass discharge valve and core discharge valve percent positons are listed. In the same table, the maximum percent scope limits observed during each stall are tabulated for the stage one vanes and core OGVs. The percent limits were calculated by assuming the overall stress levels read on the scopes were composed entirely of one of

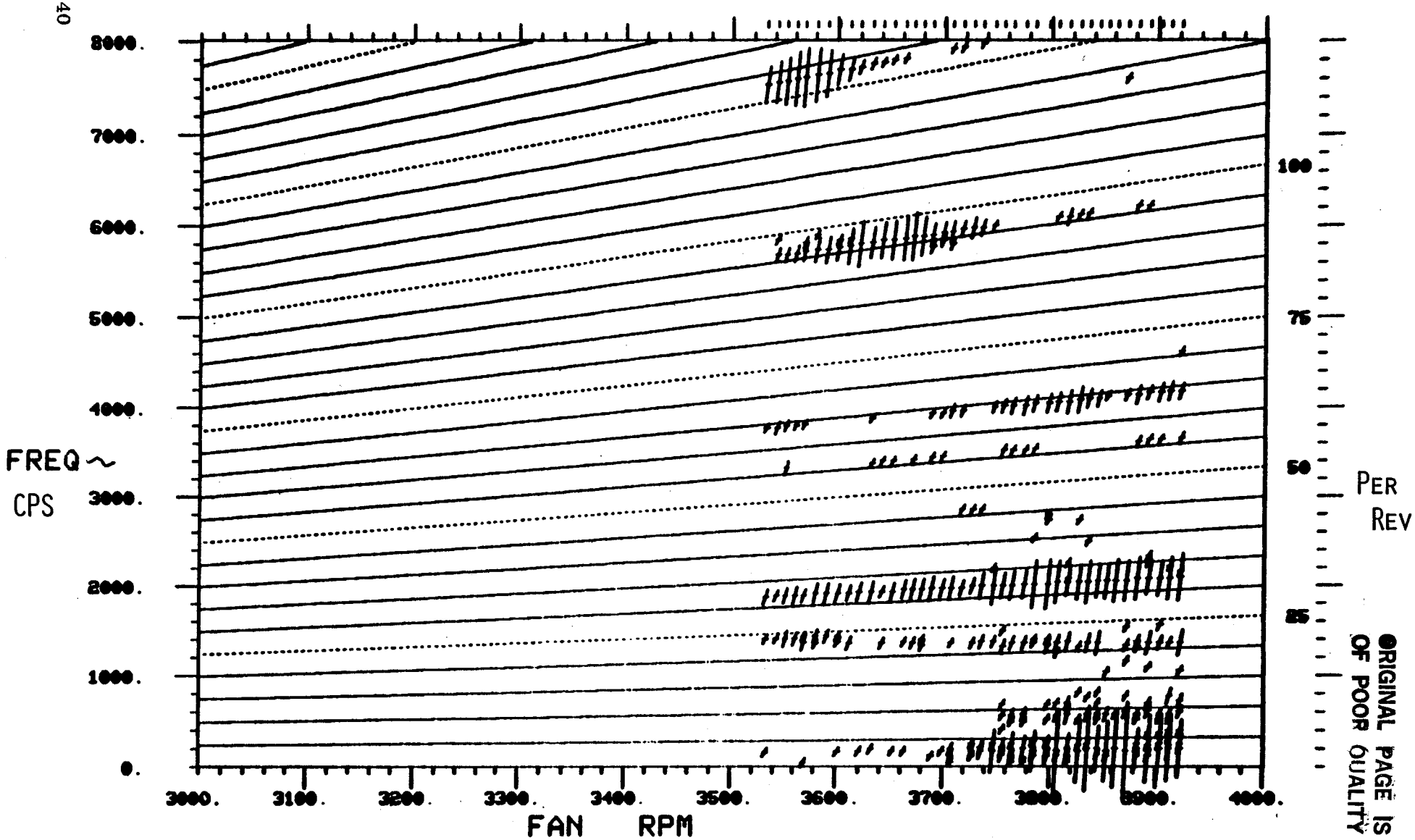

Figure 22. Campbell Diagram - Stage One Vane.

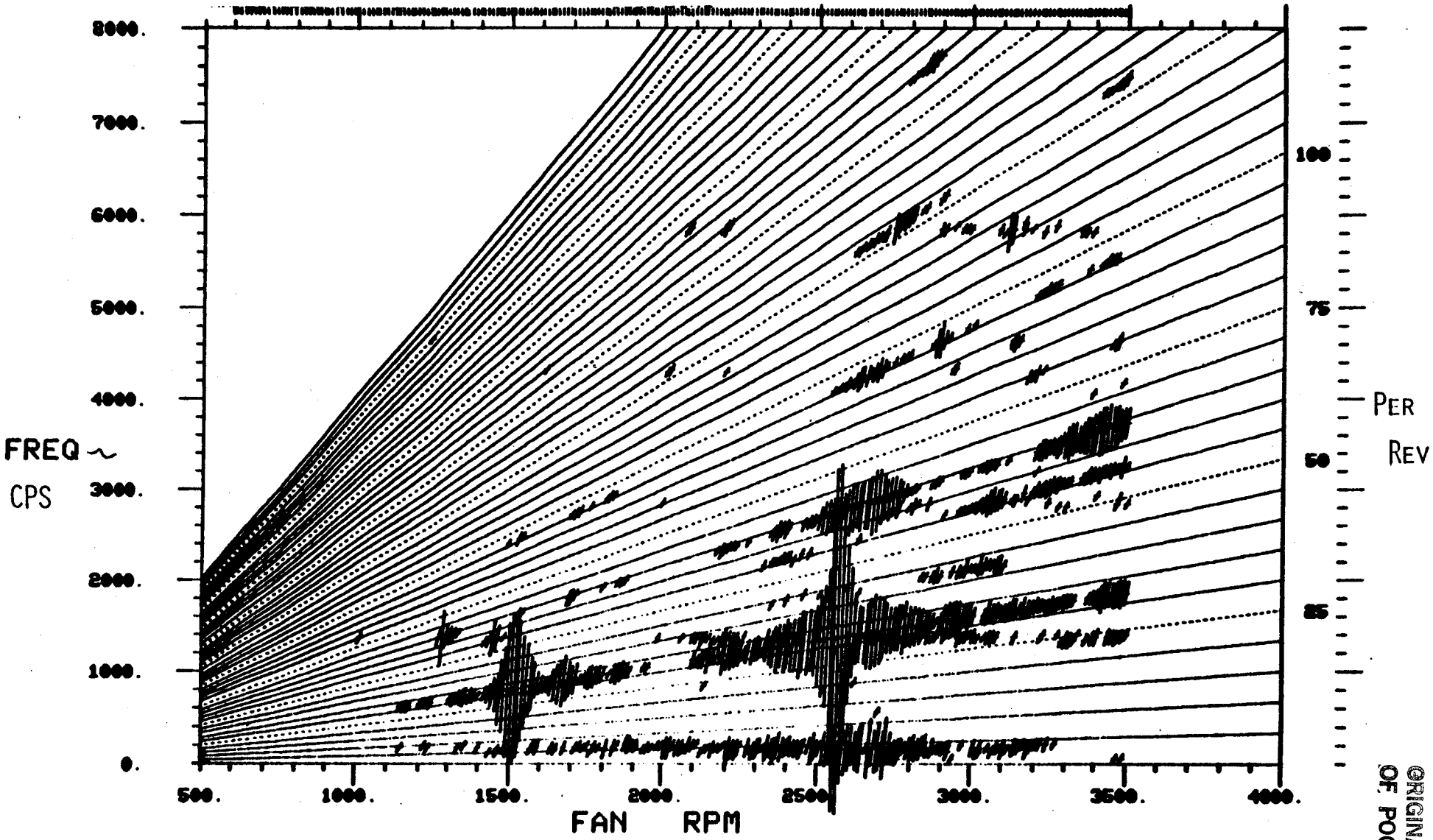

Figure 23. Campbell Diagram - Stage One Vane.

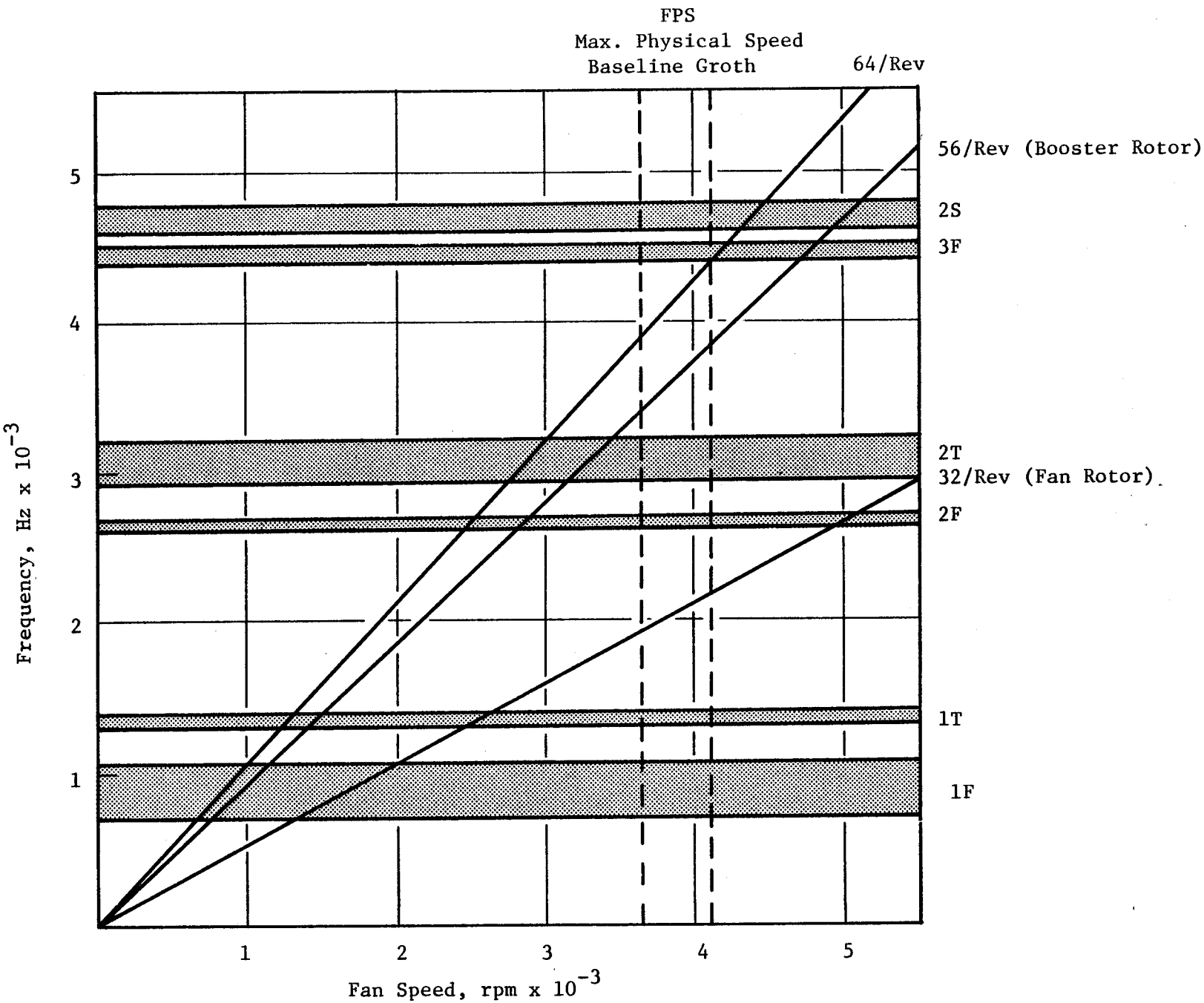

Figure 24. Campbell Diagram - Stage 1 Vane - Bench Test.

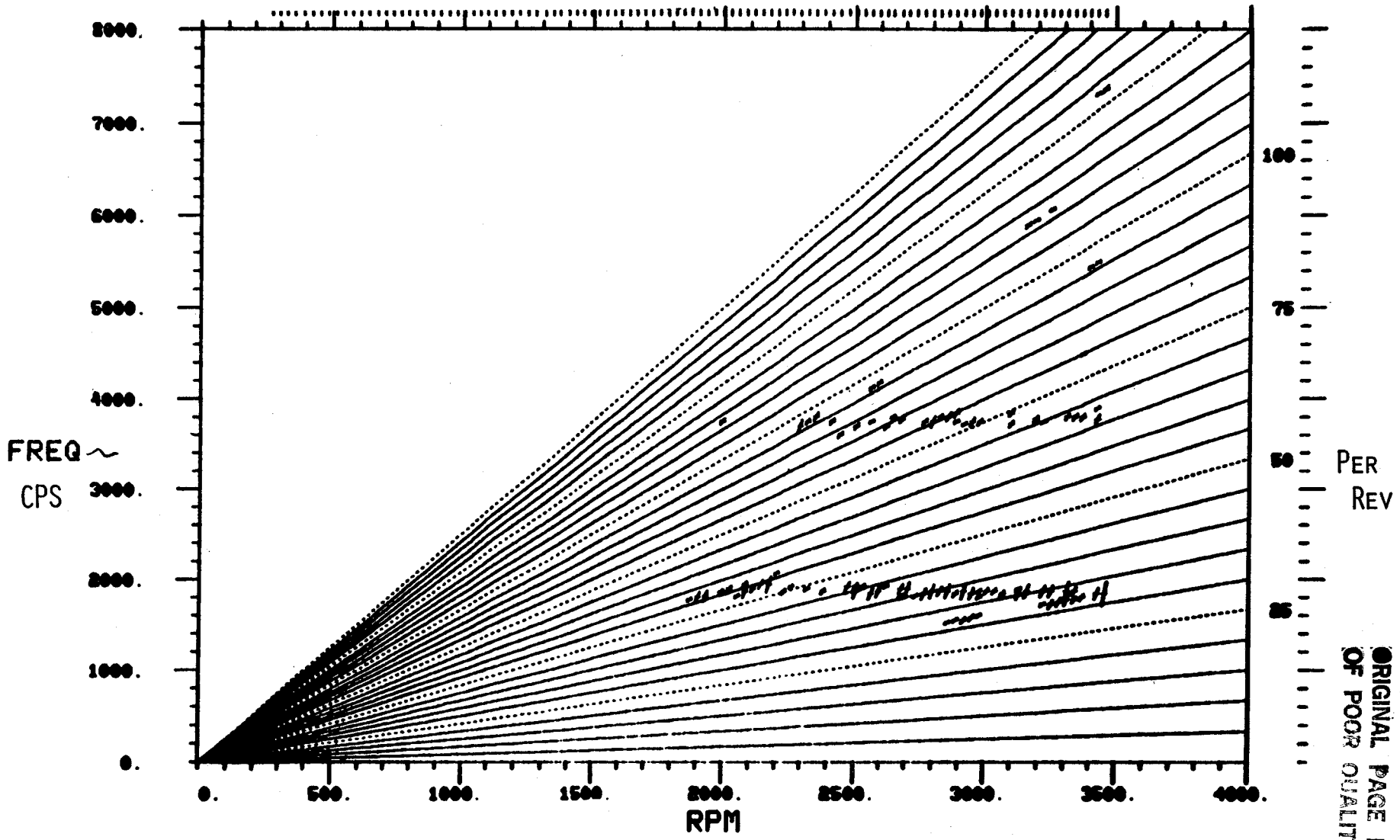

Figure 25. Campbell Diagram - Core Outlet Guide Vane - Test Data.

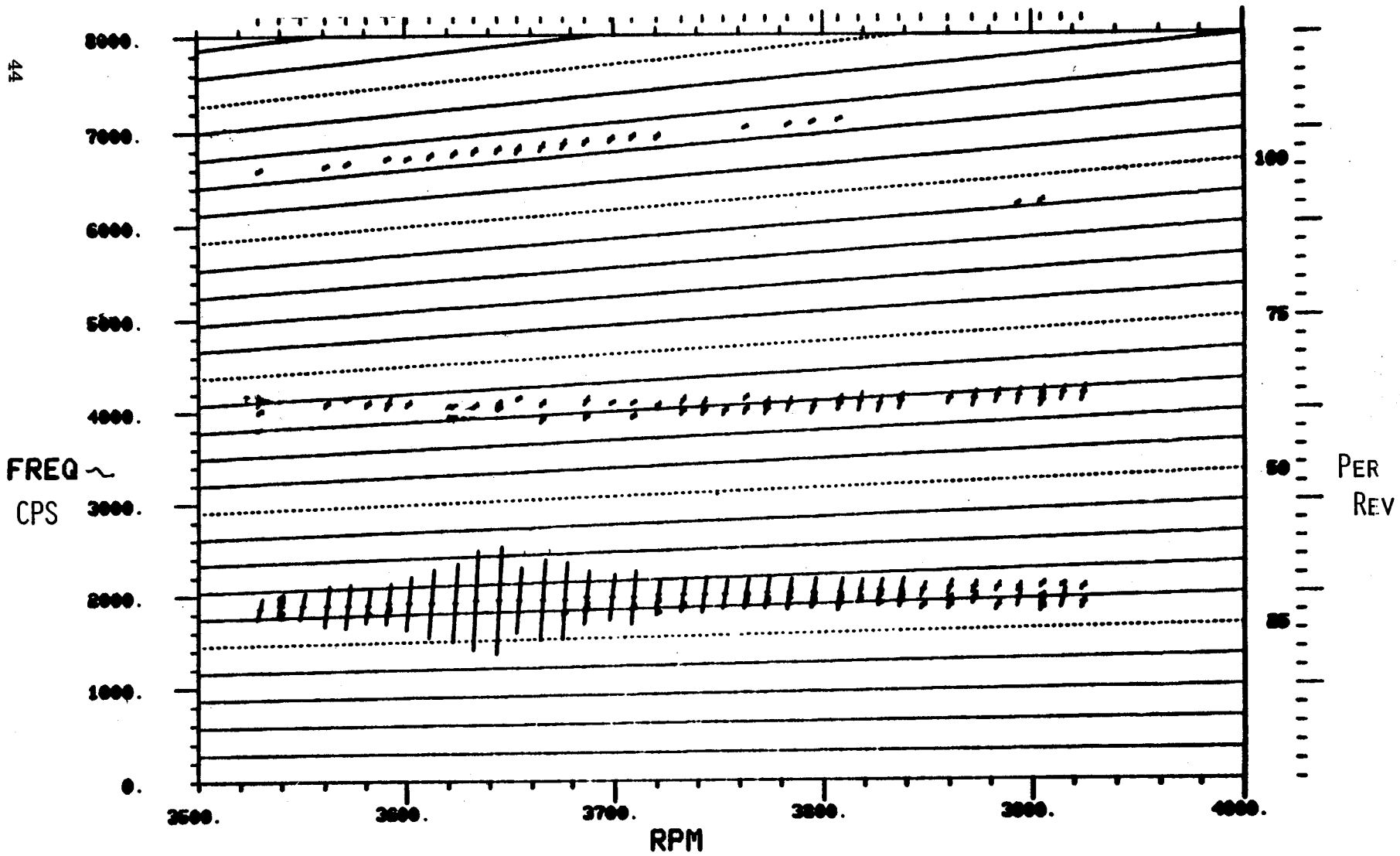

Figure 26. Campbell Diagram - Core Outlet Guide Vane - Test Data.

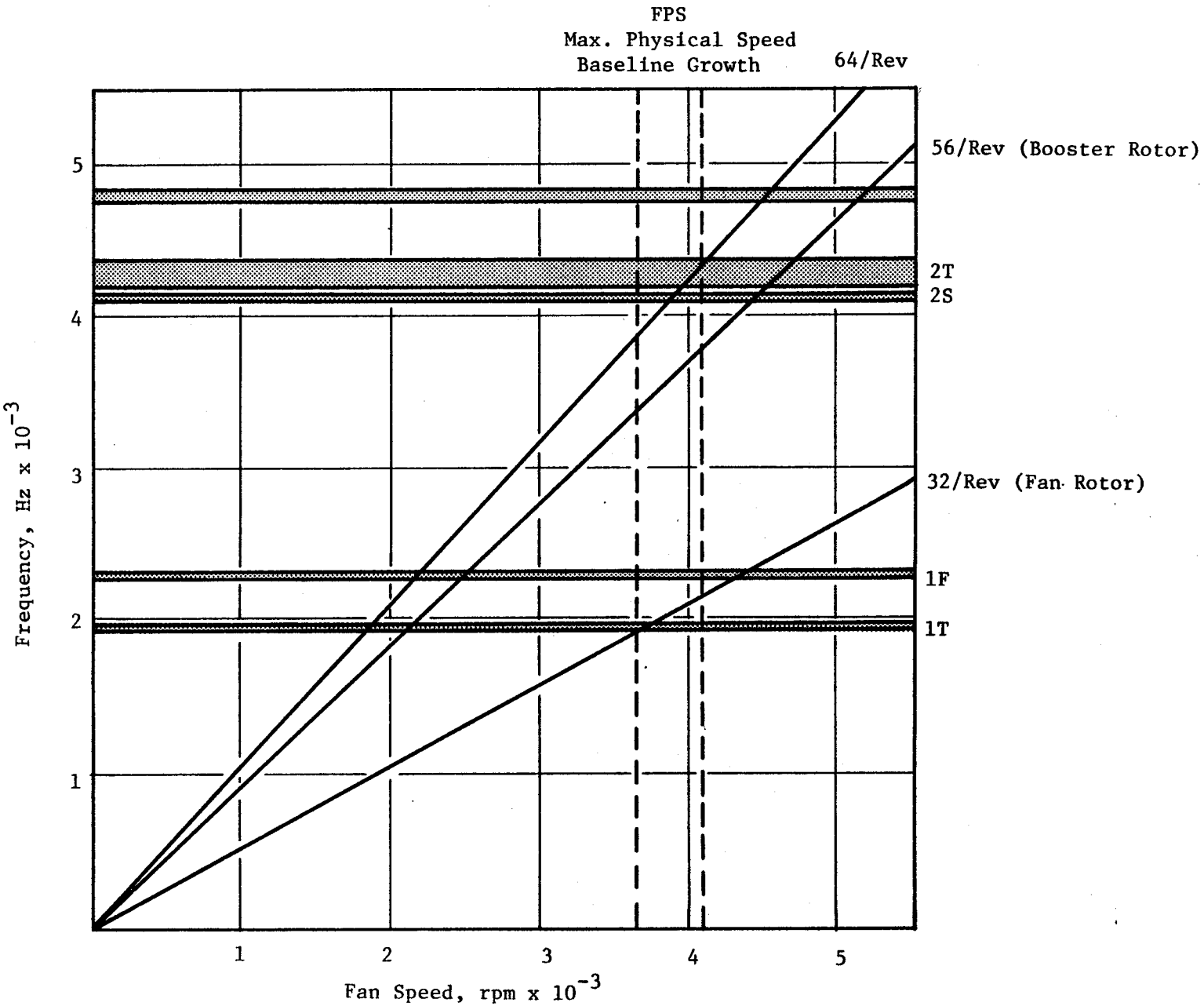

Figure 27. Campbell Diagram - Core Outlet Vane - Bench Test.

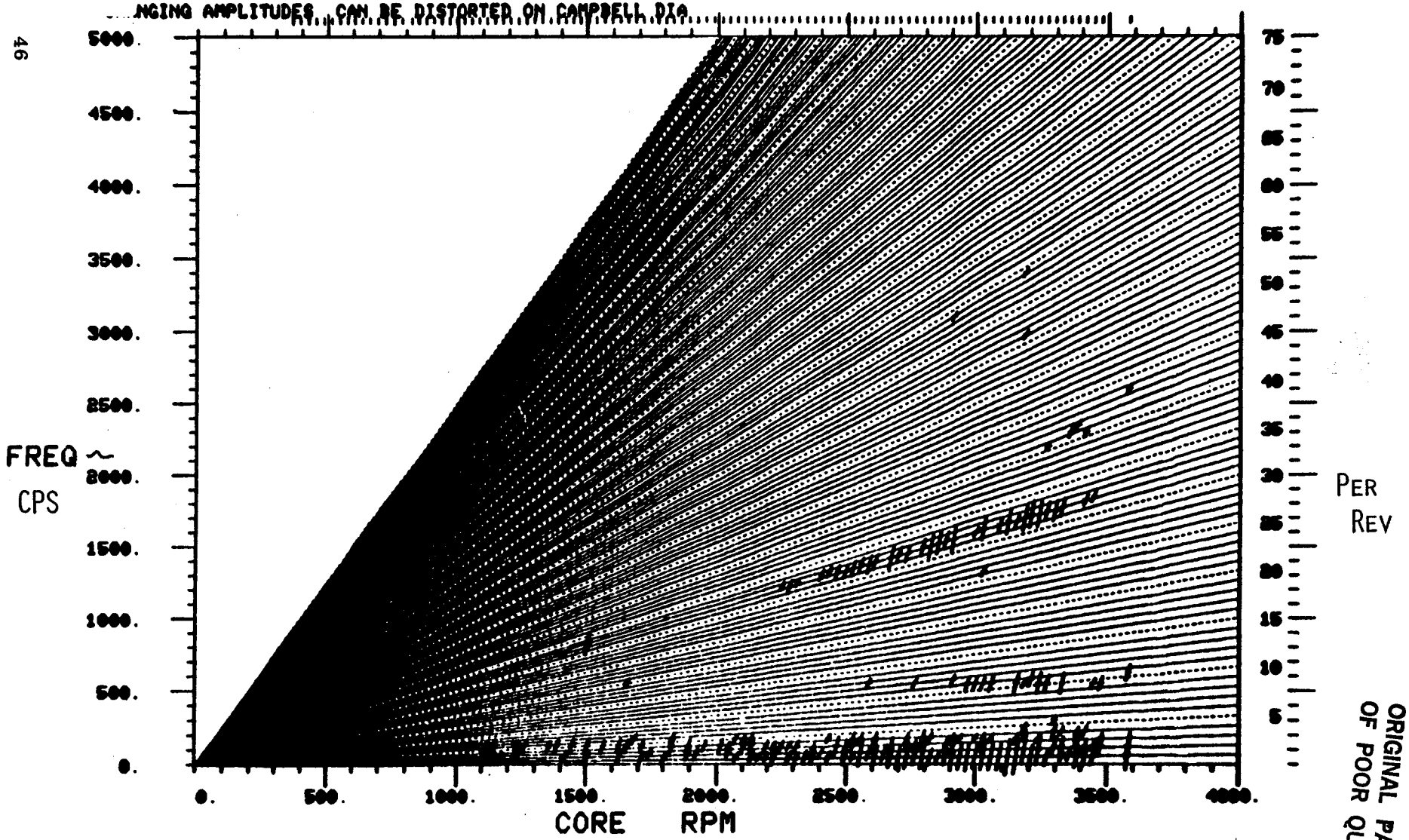

Figure 28. Campbell Diagram - Bypass Outlet Guide Vane - Test Data.

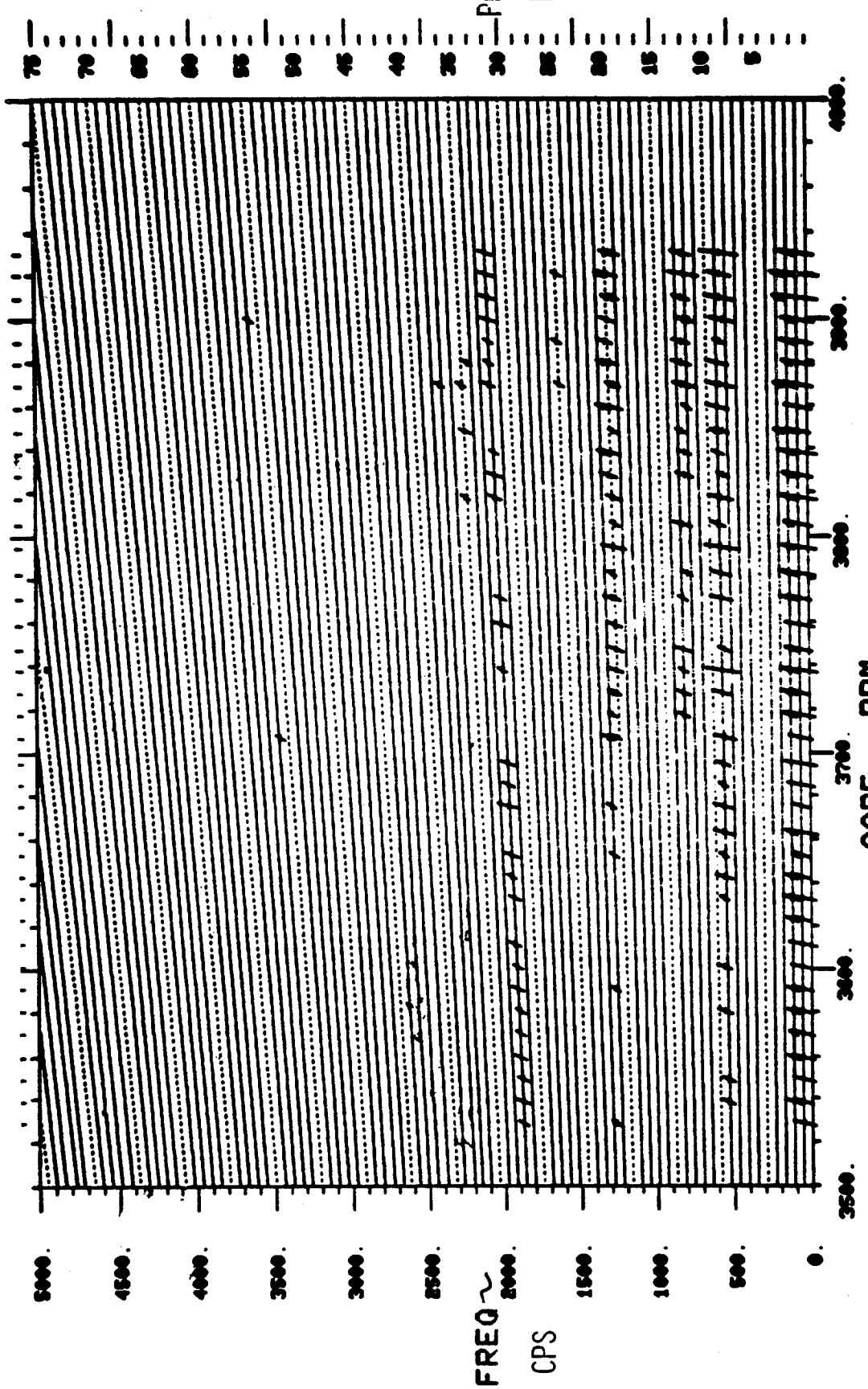

Figure 29. Campbell Diagram - Bypass Outlet Guide Vane - Test Data.

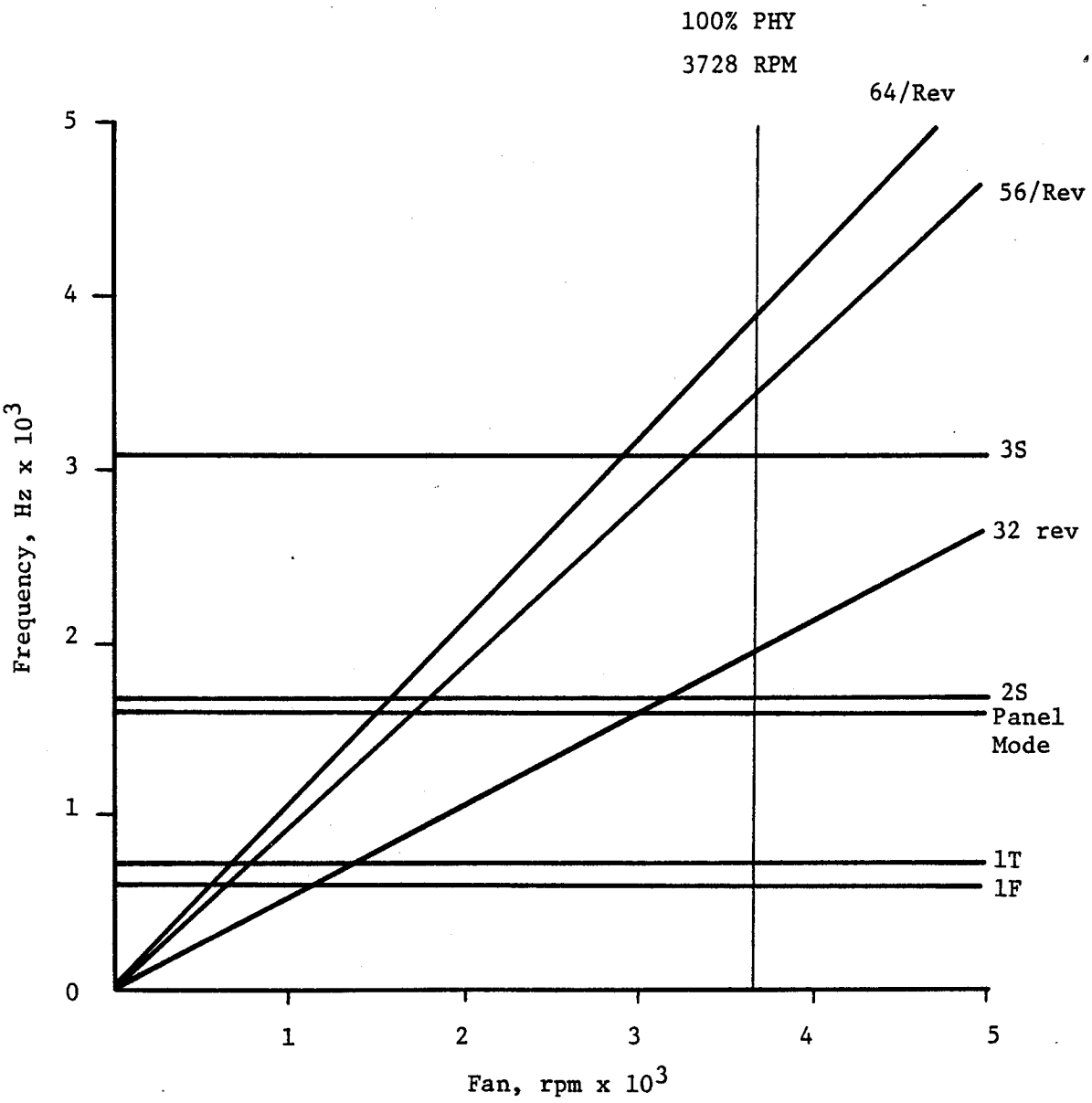

Figure 30. Campbell Diagram - Bypass Outlet Guide Vane - (Nominal Camber) - Bench Test.

Table IV. FSFT Vane Stall Events.

Stall Event	%Nc	RPM	MDV % Pos.	BDV % Pos.	Max Vane Response % Limits		
					Stage 1	OGV	Bypass
1	40	1481	40	17.0	12	20	See
2	50	1854	50	17.6	12	17	Note
3	60	2219	50	18.8	15	20	(3)
4	70	2612	60	24.8	23	27	
5	80	2968	50	25.2	24	42	
6	85	3178	64	28.3	27	43	
7	90	3345	75	29.2	33	62	
8	90	3360	100	29.0	30	73	
9	90	3360	56	29.7	27	67	
10	90	3360	56	31.0 (1)	28	63	
11	95	3550	70	31.2	28	75	
12	95	3535	60	30.0	28	67	
13	95	3535	100	32.7	31	63	
14	100	3732	75.4 (2)	100.0	47	77	45

Notes

1 Unintentional Stall - Bypass Discharge Valve (BDV) Closed in Error

2 Unintentional Stall - Main Discharge Vavel (MDV) Closed in Error

3 Except for Event 14, Response is Negligible

the vane primary modes. A nodal analysis of the strain gage signals determined that 75 to 100% of the overall stresses were in primary modes. For this reason, the percent limits recorded in Table IV are assumed to be conservative.

Time histories of representative channels during stall events are presented in Figures 31 through 33. These figures show twenty to sixty seconds of data versus signal frequencies and frequency amplitudes. Only the relative amplitudes between frequencies are usable due to the instability of this data reduction method to process rapidly changing amplitude levels. These figures confirm that a high percentage of the overall stress response was contributed by a single vibratory mode. For the core OGVs, this mode was first torsion. The stage one vanes responded to the stall at 160 Hz while the bypass OGVs responded at 80 HZ.

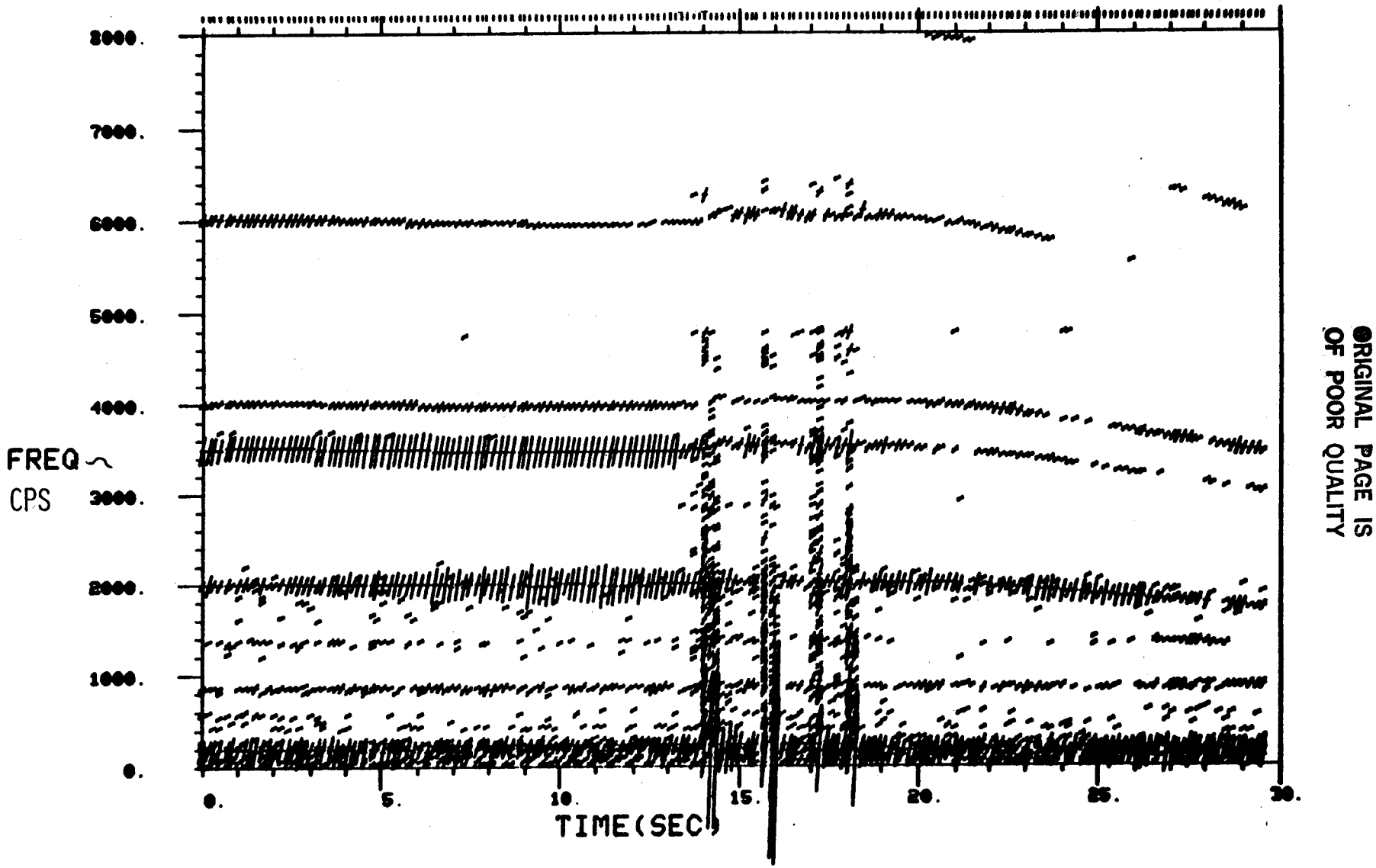

Figure 31. Stage One Vane Stall Event.

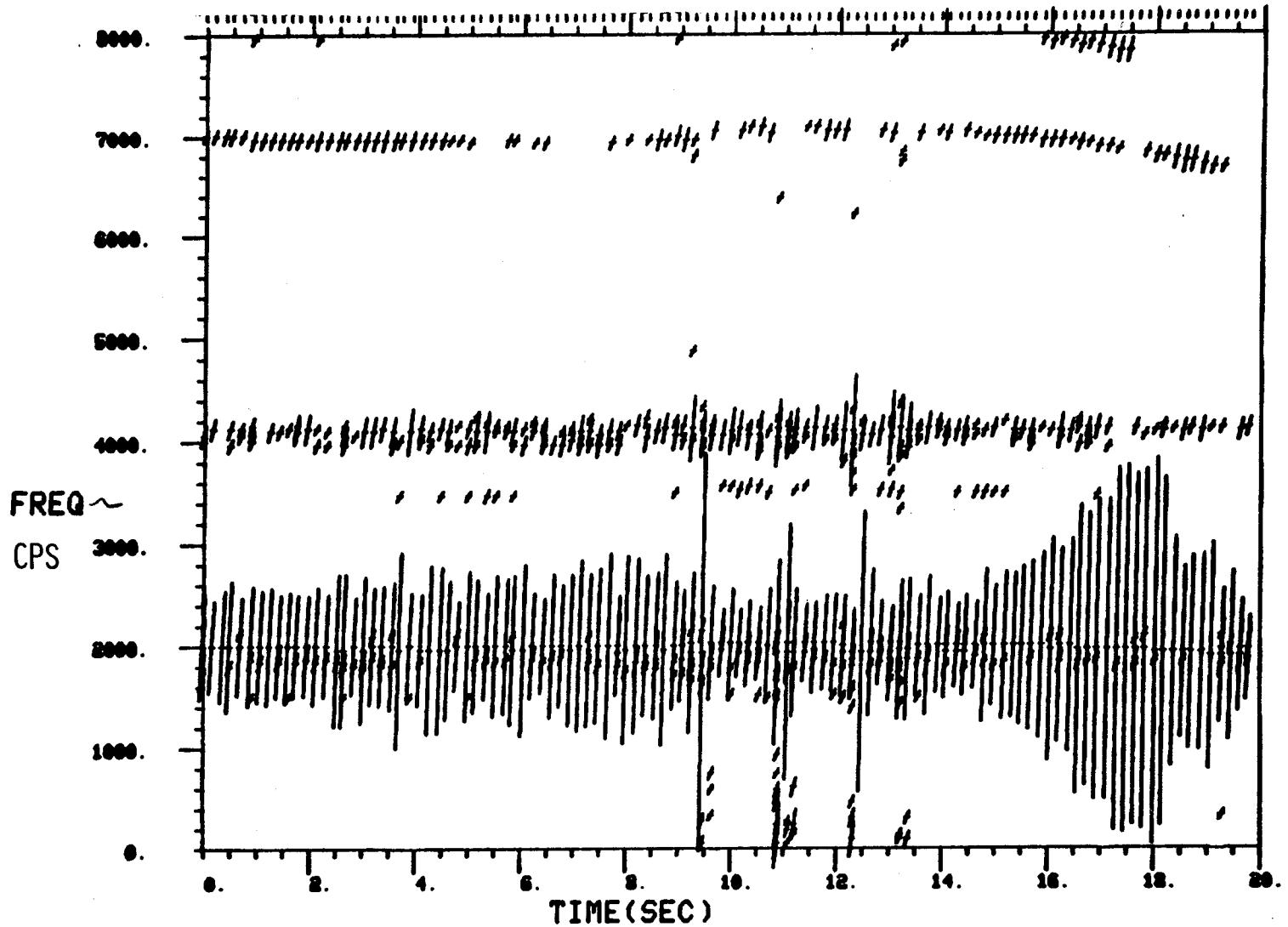

Figure 32. Core OGV Stall Event.

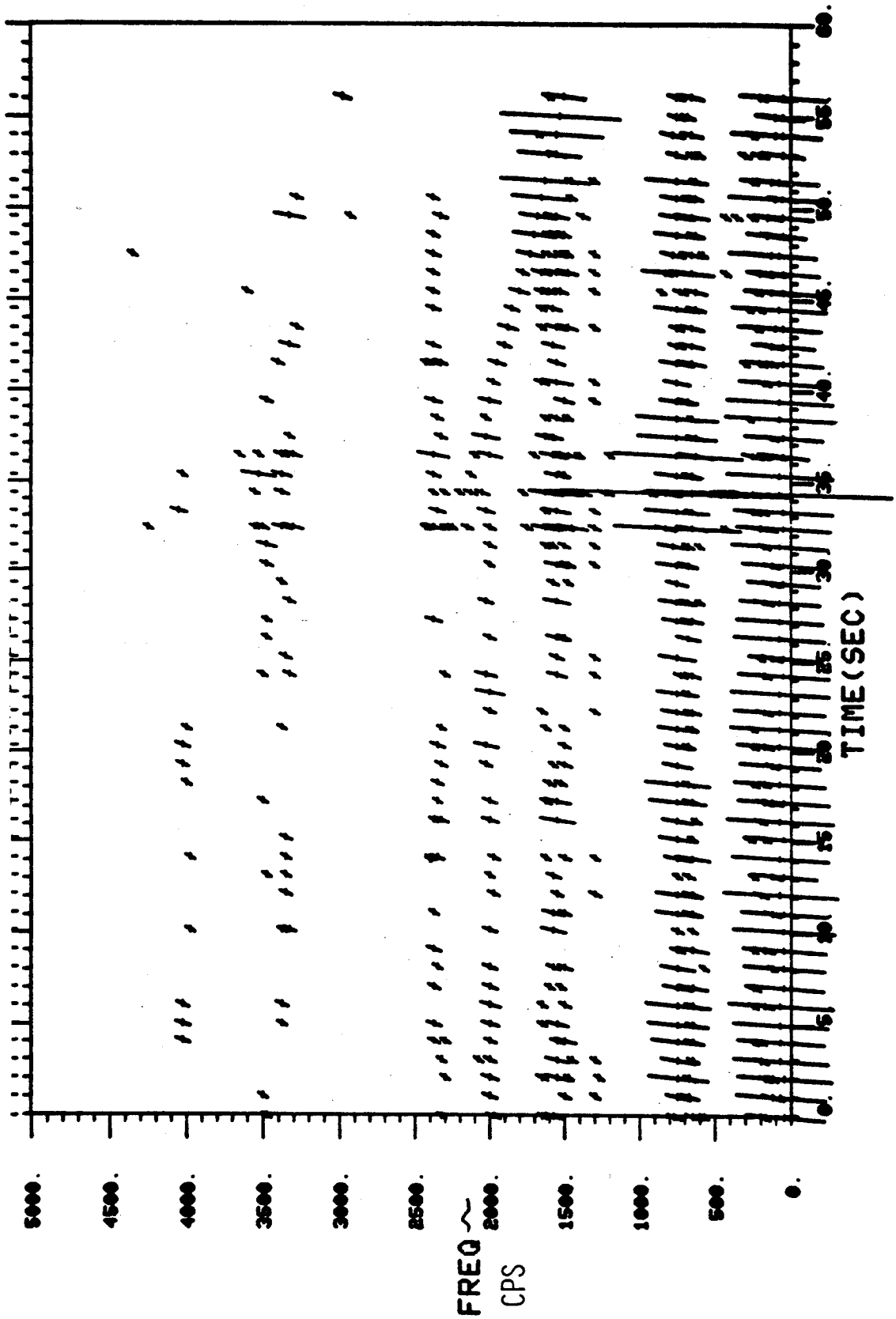

Figure 33. Bypass Outlet Guide Vane Stall Event.

SECTION VI

SYSTEM VIBRATION

The E^3 Full Scale Fan Test was completed with acceptable synchronous vibration levels throughout the entire speed range following a successful field balance of the stage one fan rotor. A field balance was required due to higher than anticipated synchronous vibration levels of the boiler-plate outer-duct facility hardware located between the fan frame and the aft-mount plane.

Thirteen (13) accelerometers were used to continuously monitor the vibration characteristics of the test vehicle. Locations of the accelerometers are defined in Table V. Signals from the accelerometers were continuously monitored on oscilloscopes and simultaneously recorded on magnetic tape. A spectrum analyzer and two X-Y plotters with tracking filters were used at the test site to further evaluate the vibration characteristics in real time.

Table V. Accelerometers Locations.

No. 1 Bearing	- Vertical, Horizontal and Axial
No. 2 Bearing	- Vertical and Horizontal
Containment Case	- Vertical and Horizontal
Fan Frame	- Vertical and Horizontal
Quarter-Stage Island	- Vertical and Horizontal
Fan Outer Duct Access Case	- Vertical and Horizontal

Synchronous vibration levels observed during the initial mechanical checkout were higher than had been predicted by the pre-test analysis. When the fan rotor was field balanced the vibration levels were reduced to an acceptable level. Figure 34 illustrates the synchronous response at the access case aft flange - horizontal accelerometer as recorded on the X-Y plotter during the last test run on an accel from 500 rpm to 3750 rpm. The accelerometer was located at the highest response location on the vehicle. At 3500 rpm, steady-state synchronous levels of 3 mils -DA and 4 mils -DA were recorded, respectively, at the forward bearing horizontal and containment case horizontal accelerometers during the final test run.

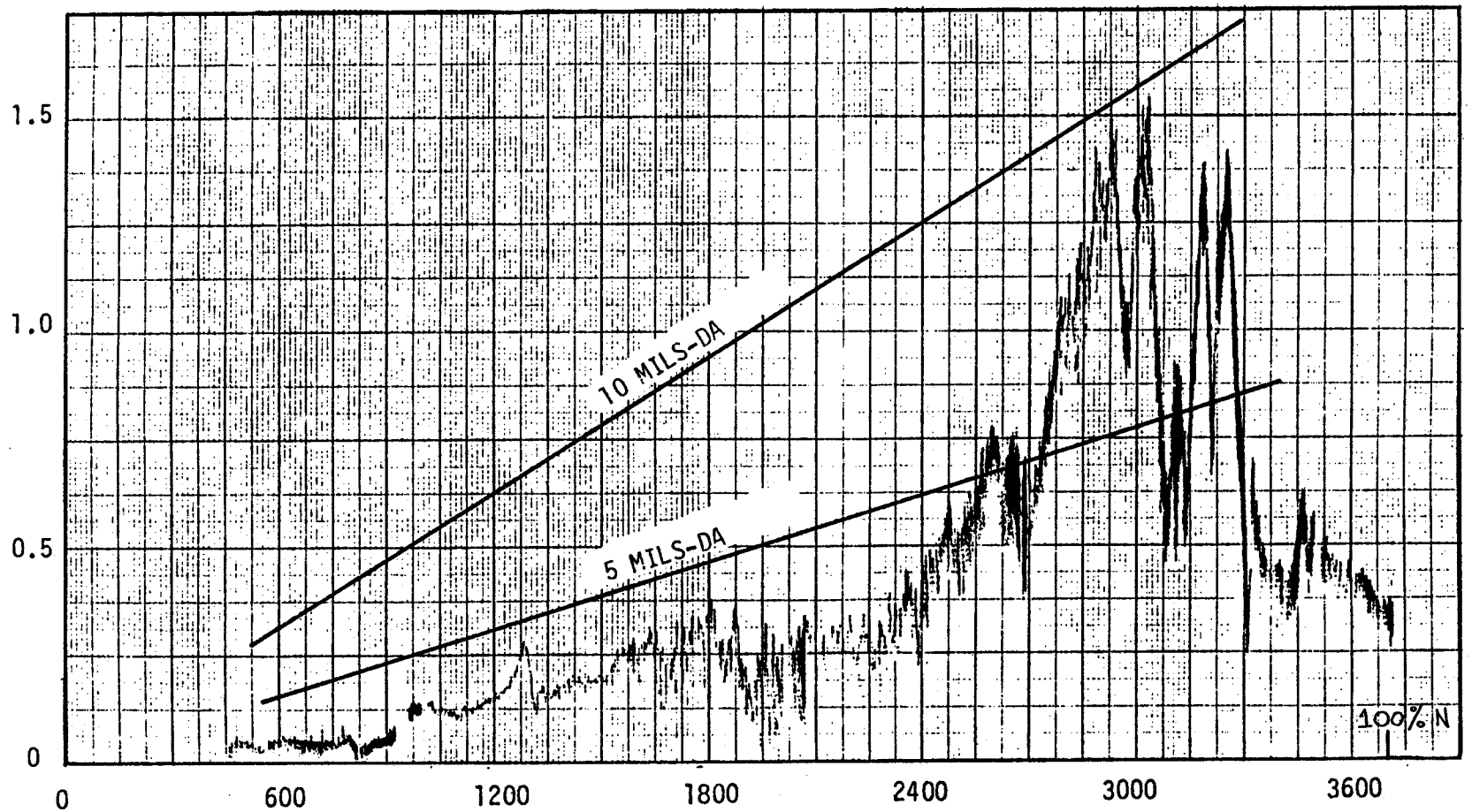

ACCESS CASE AFT FLANGE - HORIZONTAL
CONTINUOUS ACCEL STARTING AT 14:23 HOURS

Figure 34. Full Scale Test Run #10 Synchronous Vibration Response at the Fan Outer Duct.

Post-test analyses were performed to determine why the response characteristics did not correlate with the pre-test analysis. The dynamic analysis computer model mass and flexibility characteristics were reviewed and refined. A parametric study was conducted where the fan frame and fan rotor mass and flexibility properties were varied to determine the sensitivity of the characteristic fan nodding mode. This mode is typical of all high bypass turbofan engines and involves mass coupling of the rotor with strain energy in the fan frame. The post-test analysis indicated that the characteristic mode should be closer to 5200 rpm than 5450 rpm as originally predicted, but still far above the normal speed range. This verified that the high response at 3000 rpm was not associated with the characteristic fan nodding mode. This high response has been attributed to the influence of the Lynn facility shafting between the thrust bearing and the gearbox. Therefore, similar vibration problems associated with the a fan rotor unbalance are not anticipated for the ICLS test program.

SECTION VII
CONCLUSIONS

A summary of the fan bypass (with adjustments) and core-stream performance at the important engine cycle conditions of max climb, max cruise, and takeoff is shown in Table VI. The fan momentum-averaged efficiencies, summarized relative to the component test goals and the fully-developed FPS fan goals, are shown in Table VII. The test efficiencies exceed the component test goals at all of the important engine operating conditions. Relative to the FPS engine goals, the fan bypass efficiency is higher by 0.7 points at max cruise and 0.5 points at max climb. At takeoff, the bypass efficiency is 0.7 point lower than the FPS goal. The core-stream efficiency is 0.7 point greater than the FPS goal at max climb, 0.3 point greater at max cruise, and 0.1 point greater at takeoff. The target stall line was exceeded at all speeds, above 40%, by approximately 3-5%. Ample stall margin is available for a high bypass ratio turbofan operating at the sea level takeoff condition. The core-steam pressure and efficiency test data profiles were very close to the design intent, demonstrating that the fan hub and quarter-stage will provide the desired flow field, as designed, at the core compressor inlet. Virtually all goals covering the bypass and core-stream performance were met or exceeded. Since the fan displayed highly-stable aeromechanical characteristics and low stresses, it was decided to use the fan component test configuration, without any modifications, for the ICLS demonstrator turbofan engine test. The high vibratory response at 3000 rpm has been attributed to the Lynn facility shafting and will not present a fan rotor unbalance problem during the ICLS test program.

Table VI. Performance Results.

Parameter	Max Climb	Max Cruise	Takeoff
Corrected Tip Speed, ft/sec	1316	1283	1175
Corrected Total Fan Airflow, lbm/sec	1420	1395	1270
Flow/Annulus Area, lbm/sec-ft^2	42.8	42.1	38.4
Bypass Total-Pressure Ratio, P14/P10	1.65	1.61	1.50
Bypass Adiabatic Efficiency (Momentum-Avg), η_{14}	0.886	0.892	0.893
Core-Stream Total-Pressure Ratio, P23/P10	1.67	1.62	1.53
Core-Stream Adiabatic Efficiency, η_{23}	0.892	0.895	0.898
Bypass Ratio	6.9	7.0	7.4

Table VII. Fan Efficiency (Momentum-Averaged) Summary.

Parameter	Max Climb	Max Cruise	Takeoff
Bypass Adiabatic Efficiency			
Full-Scale Fan Test Goal	0.869	0.877	0.890
FPS Goal	0.879	0.887	0.900
Full-Scale Fan Test (Adjusted)	0.886	0.892	0.893
Core-Stream Adiabatic Efficiency			
Full-Scale Fan Test Goal	0.875	0.882	0.887
FPS Goal	0.885	0.882	0.887
Full-Scale Fan Test Measured	0.892	0.895	0.898

SECTION VIII

REFERENCES

Ref. 1: Sullivan, T.J., Luebering. G.W., and Gravitt, R.D. "Energy Efficient Engine Fan Test Hardware Detailed Design Report," NASA CR-165148, R80AEG417, October 1980.

APPENDIX

E^3 FAN TEST DATA SUMMARY

EEE FAN + 1/4 STAGE BOOSTER RIG TEST SUMMARY ON 11/17/82 AT 14.594

RDG	PNC1ØR	* MOM-AVG FAN BYPASS DATA * W1ØADJ	P14Q1Ø	E14MOM	* MEASURED FAN BYPASS DATA * W1ØR	P14Q1Ø	E14D1Ø	* MEASURED CORE STREAM DATA * W25R1Ø	P23Q1Ø	E23D1Ø	BPR
25	39.93	639.2	1.Ø692	Ø.882Ø	638.9	1.Ø692	Ø.9Ø76	77.4	1.Ø826	Ø.9232	7.249
17	39.95	592.5	1.Ø813	Ø.9Ø14	592.3	1.Ø813	Ø.92Ø9	73.9	1.Ø919	Ø.9378	7.Ø2Ø
24	39.97	7Ø6.6	1.Ø47Ø	Ø.721Ø	7Ø6.1	1.Ø47Ø	Ø.7427	1Ø2.7	1.Ø477	Ø.6358	5.876
1Ø2	39.97	5Ø6.Ø	1.Ø89Ø	Ø.8281	5Ø5.5	1.Ø89Ø	Ø.8425	65.6	1.Ø984	Ø.9ØØ1	6.7Ø5
45	4Ø.Ø4	425.Ø	1.Ø9Ø3	Ø.7397	424.9	1.Ø9Ø3	Ø.7554	46.2	1.1Ø27	Ø.8574	8.2ØØ
97	49.98	757.7	1.1269	Ø.8943	757.1	1.1269	Ø.9Ø79	93.5	1.1432	Ø.9Ø15	7.1Ø1
1Ø3	49.99	652.1	1.1417	Ø.8447	651.7	1.1417	Ø.8555	8Ø.7	1.1564	Ø.8979	7.Ø78
46	5Ø.Ø1	7Ø7.2	1.137Ø	Ø.8885	7Ø6.7	1.137Ø	Ø.8958	89.6	1.151Ø	Ø.9Ø82	6.891
26	5Ø.Ø3	798.1	1.1111	Ø.8579	797.4	1.1111	Ø.87Ø2	95.1	1.1334	Ø.8761	7.385
47	5Ø.17	547.2	1.145Ø	Ø.742Ø	547.Ø	1.145Ø	Ø.7535	72.Ø	1.1657	Ø.8654	6.596
1Ø4	5Ø.22	866.Ø	1.Ø794	Ø.8144	865.Ø	1.Ø794	Ø.8251	1Ø9.5	1.1Ø9Ø	Ø.8Ø78	6.9ØØ
33	59.95	1Ø19.3	1.1174	Ø.75Ø9	1Ø17.6	1.1174	Ø.7544	141.9	1.1223	Ø.6814	6.17Ø
1Ø5	6Ø.Ø5	911.2	1.1868	Ø.9Ø17	91Ø.Ø	1.1868	Ø.9Ø42	113.5	1.2Ø99	Ø.8889	7.Ø16
27	6Ø.Ø6	99Ø.9	1.14Ø4	Ø.8222	989.3	1.14Ø4	Ø.8237	125.3	1.1719	Ø.8415	6.898
86	6Ø.Ø7	959.3	1.1631	Ø.8678	957.9	1.1631	Ø.8685	118.6	1.1966	Ø.8739	7.Ø77
87	6Ø.Ø7	853.7	1.2Ø37	Ø.89Ø1	852.8	1.2Ø37	Ø.8922	1Ø7.Ø	1.2242	Ø.9Ø19	6.969
49	6Ø.13	792.2	1.2123	Ø.8565	791.5	1.2123	Ø.86Ø5	92.7	1.2358	Ø.8987	7.54Ø
48	6Ø.14	669.2	1.2132	Ø.7555	668.8	1.2132	Ø.7612	85.1	1.2438	Ø.8841	6.955
11Ø	69.87	865.7	1.3Ø22	Ø.819Ø	864.7	1.3Ø22	Ø.8249	11Ø.7	1.3354	Ø.8943	6.8Ø9
111	69.89	8Ø2.6	1.2963	Ø.756Ø	8Ø1.8	1.2963	Ø.763Ø	1Ø8.1	1.3394	Ø.8863	6.415
79	69.93	1Ø32.1	1.2776	Ø.8925	1Ø3Ø.3	1.2776	Ø.8959	123.7	1.3127	Ø.9ØØ5	7.332
81	69.97	925.2	1.3ØØ4	Ø.8526	924.1	1.3ØØ4	Ø.8606	115.4	1.3311	Ø.9Ø71	7.ØØ9
83	69.99	1Ø92.8	1.2442	Ø.8778	1Ø9Ø.6	1.2442	Ø.8811	152.8	1.2589	Ø.8493	6.138
22	7Ø.Ø4	1Ø51.Ø	1.2695	Ø.8988	1Ø49.1	1.2695	Ø.8997	129.5	1.3Ø64	Ø.9Ø52	7.1Ø2
28	7Ø.Ø8	1124.5	1.2Ø13	Ø.786Ø	1122.2	1.2Ø13	Ø.7929	123.7	1.2755	Ø.8737	8.Ø74

EEE FAN + 1/4 STAGE BOOSTER RIG TEST SUMMARY ON 11/17/82 AT 14.594

RDG	PNC1ØR	* MOM-AVG FAN BYPASS DATA * W1ØADJ	P14Q1Ø	E14MOM	* MEASURED FAN BYPASS DATA * W1ØR	P14Q1Ø	E14D1Ø	* MEASURED CORE STREAM DATA * W25R1Ø	P23Q1Ø	E23D1Ø	BPR
8Ø	7Ø.Ø9	967.8	1.2968	Ø.8712	966.4	1.2968	Ø.8776	116.6	1.3269	Ø.9Ø14	7.285
32	7Ø.15	1151.6	1.1598	Ø.68Ø6	1149.Ø	1.1598	Ø.6836	157.3	1.1812	Ø.6974	6.3Ø5
52	79.93	918.8	1.3985	Ø.7469	917.6	1.3985	Ø.7517	1Ø2.7	1.4492	Ø.8494	7.935
152	8Ø.ØØ	1Ø24.2	1.4191	Ø.8226	1Ø22.5	1.4191	Ø.8291	139.1	1.45Ø9	Ø.8951	6.349
31	8Ø.Ø4	1259.4	1.2318	Ø.6777	1255.8	1.2318	Ø.6756	17Ø.5	1.2794	Ø.7594	6.364
5Ø	8Ø.Ø5	1221.Ø	1.3561	Ø.8877	1217.8	1.3561	Ø.89Ø1	144.4	1.4Ø5Ø	Ø.8997	7.436
15Ø	8Ø.Ø7	1176.8	1.3891	Ø.8976	1174.Ø	1.3891	Ø.8968	143.9	1.4225	Ø.9Ø61	7.158
29	8Ø.Ø9	1242.4	1.2684	Ø.7176	1238.8	1.2684	Ø.7274	137.1	1.39Ø2	Ø.8854	8.Ø33
151	8Ø.18	11Ø9.8	1.4179	Ø.8669	11Ø7.5	1.4179	Ø.8742	135.9	1.444Ø	Ø.9ØØ3	7.148
75	84.83	1Ø92.7	1.4866	Ø.8261	1ØØØ.5	1.4866	Ø.8358	13Ø.4	1.5226	Ø.8824	7.366
77	84.9Ø	1311.7	1.29Ø9	Ø.7Ø63	13Ø7.5	1.29Ø9	Ø.71Ø7	177.4	1.34Ø2	Ø.7762	6.368
74	85.Ø2	1159.1	1.4911	Ø.8611	1156.5	1.4911	Ø.87Ø5	138.7	1.5163	Ø.8912	7.34Ø
53	85.Ø4	1297.2	1.4Ø34	Ø.8691	1293.2	1.4Ø34	Ø.8719	156.6	1.4583	Ø.8898	7.256
71	85.Ø4	1271.1	1.4387	Ø.8968	1267.3	1.4387	Ø.8966	154.3	1.4787	Ø.8993	7.213
72	85.Ø5	1248.2	1.4565	Ø.8945	1244.7	1.4565	Ø.8947	146.4	1.49Ø9	Ø.8965	7.499
73	85.Ø6	12Ø6.Ø	1.4791	Ø.8814	12Ø2.9	1.4791	Ø.8867	143.5	1.5Ø44	Ø.8944	7.38Ø
115	85.52	1ØØ7.7	1.4666	Ø.75Ø4	1ØØ6.1	1.4666	Ø.7549	138.9	1.5324	Ø.8911	6.241
1Ø6	89.92	1359.Ø	1.3461	Ø.7836	1354.2	1.3461	Ø.7841	168.1	1.49Ø9	Ø.9ØØØ	7.Ø57
92	9Ø.ØØ	1191.1	1.5737	Ø.8343	1188.2	1.5737	Ø.8439	152.4	1.5976	Ø.893Ø	6.798
91	9Ø.Ø1	1124.2	1.5562	Ø.7958	1121.8	1.5562	Ø.8Ø19	14Ø.6	1.6Ø26	Ø.8787	6.977
55	9Ø.Ø5	1357.Ø	1.4991	Ø.8947	1352.2	1.4991	Ø.896Ø	171.1	1.5348	Ø.9Ø26	6.9Ø5
36	9Ø.Ø6	1367.4	1.4523	Ø.8542	1362.5	1.4523	Ø.8554	165.6	1.5194	Ø.8884	7.227
68	9Ø.Ø6	1231.Ø	1.577Ø	Ø.8577	1227.7	1.577Ø	Ø.8665	155.8	1.591Ø	Ø.8953	6.88Ø
58	9Ø.Ø9	1292.5	1.5596	Ø.8876	1288.6	1.5596	Ø.8916	151.9	1.5767	Ø.8928	7.484
133	9Ø.14	1Ø54.6	1.5289	Ø.736Ø	1Ø52.7	1.5289	Ø.7383	126.5	1.6ØØ5	Ø.8555	7.319

EEE FAN + 1/4 STAGE BOOSTER RIG TEST SUMMARY ON 11/17/82 AT 14.594

RDG	PNC1ØR	* MOM-AVG FAN BYPASS DATA * W1ØADJ	P14Q1Ø	E14MOM	* MEASURED FAN BYPASS DATA * W1ØR	P14Q1Ø	E14D1Ø	* MEASURED CORE STREAM DATA * W25R1Ø	P23Q1Ø	E23D1Ø	BPR
126	9Ø.15	1351.5	1.5145	Ø.8974	1346.8	1.5145	Ø.8988	184.5	1.5255	Ø.8954	6.3ØØ
144	94.75	1123.Ø	1.5988	Ø.7331	112Ø.6	1.5988	Ø.7364	139.4	1.6747	Ø.86Ø1	7.Ø36
64	95.ØØ	1263.Ø	1.6523	Ø.8851	1358.1	1.6523	Ø.8898	165.5	1.6535	Ø.8912	7.2Ø4
96	95.ØØ	1278.8	1.6682	Ø.838Ø	1275.Ø	1.6682	Ø.846Ø	161.7	1.6785	Ø.89Ø7	6.885
62	95.Ø9	14ØØ.Ø	1.5848	Ø.8898	1394.5	1.5848	Ø.889Ø	173.4	1.6211	Ø.8955	7.Ø44
65	95.13	1333.2	1.664Ø	Ø.866Ø	1328.7	1.664Ø	Ø.8746	162.9	1.667Ø	Ø.8919	7.155
135	95.13	141Ø.3	1.5777	Ø.8837	14Ø4.7	1.5777	Ø.8838	193.3	1.5945	Ø.8879	6.268
63	95.15	1388.5	1.6162	Ø.8932	1383.3	1.6162	Ø.8929	16Ø.4	1.6416	Ø.8861	7.623
59	95.18	14Ø7.1	1.5669	Ø.8811	14Ø1.5	1.5669	Ø.8833	193.9	1.5878	Ø.89Ø1	6.229
1ØØ	95.23	1226.8	1.6555	Ø.8Ø28	1223.6	1.6555	Ø.8Ø75	161.6	1.6883	Ø.8878	6.571
153	97.78	1427.3	1.6463	Ø.8824	1421.4	1.6463	Ø.882Ø	179.6	1.6685	Ø.8918	6.914
94	99.98	1422.1	1.735Ø	Ø.8729	1416.3	1.735Ø	Ø.8755	166.9	1.7478	Ø.8858	7.484
39	1ØØ.Ø5	1448.7	1.6615	Ø.8725	1442.4	1.6615	Ø.87ØØ	187.3	1.7Ø43	Ø.8954	6.7Ø3
117	1ØØ.1Ø	1352.6	1.7692	Ø.8427	1347.9	1.7692	Ø.8421	163.2	1.776Ø	Ø.8824	7.261
95	1ØØ.11	1395.7	1.765Ø	Ø.8643	139Ø.3	1.765Ø	Ø.8644	156.2	1.7717	Ø.879Ø	7.9ØØ
1Ø9	1ØØ.12	14Ø9.3	1.7456	Ø.8823	14Ø3.7	1.7456	Ø.8795	149.1	1.763Ø	Ø.8695	8.413
6Ø	1ØØ.13	1442.7	1.6382	Ø.8585	1436.5	1.6382	Ø.8585	2Ø1.1	1.6686	Ø.8842	6.145
88	1ØØ.27	1436.7	1.6983	Ø.8735	143Ø.6	1.6983	Ø.8739	2Ø1.2	1.7Ø88	Ø.899Ø	6.111
119	1Ø4.81	1457.4	1.7745	Ø.8446	145Ø.9	1.7745	Ø.8475	13Ø.7	1.8213	Ø.8874	7.Ø31
61	1Ø5.32	1466.2	1.7175	Ø.8331	1459.5	1.7175	Ø.8325	196.2	1.8Ø12	Ø.8846	6.44Ø

EEE FAN + 1/4 STAGE BOOSTER RIG TEST SUMMARY ON 11/17/82 AT 14.594

RDG	PNC1ØR	* MEASURED FAN BYPASS DATA * W1ØR	P14Q1Ø	E14D1Ø	* MEASURED CORE STREAM DATA * W25R1Ø	P23Q1Ø	E23D1Ø	BPR
		* * * * * BYPASS RATIO EXCURSION DATA * * * * *						
12Ø	89.97	1338.5	1.5145	Ø.9ØØ1	184.5	1.5242	Ø.8882	6.255
124	9Ø.12	1291.6	1.5366	Ø.6819	113.4	1.57Ø1	Ø.8411	1Ø.389
127	9Ø.Ø3	1323.1	1.5373	Ø.8974	189.2	1.53Ø3	Ø.8946	5.993
128	9Ø.12	1229.3	1.5736	Ø.85Ø7	199.2	1.5486	Ø.89Ø8	5.171
129	9Ø.15	1111.1	1.5345	Ø.7551	2Ø3.5	1.5514	Ø.8889	4.459
13Ø	9Ø.19	1313.4	1.5Ø55	Ø.8749	1Ø5.8	1.5548	Ø.8314	11.415
131	9Ø.16	13Ø5.3	1.5Ø17	Ø.87ØØ	97.3	1.5384	Ø.8Ø25	12.419
134	9Ø.32	1276.1	1.5279	Ø.87ØØ	88.7	1.5212	Ø.7626	13.393
136	95.22	1396.7	1.6197	Ø.8972	198.3	1.6Ø74	Ø.8954	6.Ø44
137	95.22	137Ø.Ø	1.6227	Ø.8892	123.8	1.6447	Ø.8444	1Ø.Ø66
139	95.Ø6	1256.1	1.6565	Ø.8424	132.2	1.6679	Ø.8528	8.5ØØ
14Ø	94.99	1242.5	1.6494	Ø.8357	12Ø.7	1.6461	Ø.8157	9.297
142	94.99	137Ø.3	1.5794	Ø.8697	1Ø7.5	1.6Ø35	Ø.7924	11.746
143	95.Ø9	1357.3	1.5171	Ø.8834	112.2	1.6195	Ø.81Ø6	11.Ø92
145	94.91	13Ø2.3	1.66Ø9	Ø.8495	2Ø7.2	1.6266	Ø.8956	5.285
146	95.25	1249.8	1.651Ø	Ø.8Ø5Ø	212.3	1.6361	Ø.8977	4.387

ORIGINAL PAGE IS
OF POOR QUALITY

DISTRIBUTION

NASA Headquarters
600 Independence Avenue, SW
Washington, DC 20546
Attention: RTP-6/R.S. Colladay
RTP-6/C.C. Rosen
RTP-6/J. Facey
RTM-6/L. Harris

NASA-Lewis Research Center
21000 Brookpark Road
Cleveland, OH 44135

Attention:	D.L. Nored	MS 301-2
	C.C. Ciepluch	MS 301-4 (18 copies)
	J.W. Schaefer	MS 301-4
	P.G. Batterton	MS 301-4
	G.K. Sievers	MS 301-2
	M.A. Beheim	MS 3-5
	M.J. Hartmann	MS 3-7
	R.A. Rudey	MS 86-5
	W.C. Strack	MS 501-10
	T.P. Moffitt	MS 77-2
	R.E. Jones	MS 86-6
	L.J. Kiraly	MS 23-2
	D.C. Mikkelson	MS 86-1
	A. Long	MS 500-305
	J.F. Groeneweg	MS 54-3
	W.M. Braithwaite	MS 500-208
	J.C. Williams	MS 500-211
	R.L. Davies	MS 106-1
	R.H. Johns	MS 49-6
	L.J. Kaszubinski	MS 86-2
	J.F. Sellers	MS 100-1
	J.R. Mihaloew	MS 100-1
	L. Reid	MS 5-9
	D.W. Drier	MS 86-2
	R.W. Niedzwiecki	MS 86-6
	AFSC Liaison Office	MS 501-3
	ARMY R&T Propulsion Lab	MS 302-2

NASA Ames Research Center
Moffett Field, CA 94035
Attention: 202-7/M.H. Waters

NASA Langley Research Center
Langley Field, VA 23365
Attention: R. Leonard
D. Maiden
L.J. Williams

NASA Dryden Flight Research Center
P.O. Box 273
Edwards, CA 93523
Attention: J.A. Albers

Department of Defense
Washington, DC 20301
Attention: R. Standahar 3D1089 Pentagon

Wright-Patterson Air Force Base
Dayton, OH 45433
Attention: APL Chief Scientist
E.E. Abell
H.I. Bush
E.E. Bailey (NASA Liaison)
R.P. Carmichael
R. Ellis
W.H. Austin, Jr.

AFWAL/PS
ASD/YZE
AFWAL/POT
AFWAL/NASA
ASD/XRHI
ASD/YZN
ASD/ENF

Eustis Directorate
U.S. Army Air Mobility
R&D Laboratory
Fort Eustis, VA 23604
Attention: J. Lane, SAVDL-EU-Tapp

NAVY Department
Naval Air Systems Command
Washington, DC 20361
Attention: W. Koven AIR-03E
J.L. Byers AIR-53602
E.A. Lichtman AIR-330E
G. Derderian AIR-5362C

NAVAL Air Propulsion Test Center
Trenton, NJ 08628
Attention: J.J. Curry
A.A. Martino

U.S. Naval Air Test Center
Code SY-53
Patuxent River, MD 20670
Attention: E.A. Lynch

USAVRAD Command
P.O. Box 209
St. Louis, MO 63166
Attention: Robert M. Titus

Detroit Diesel Allison Div. G.M.C.
333 West First St.
Dayton, OH 45202
Attention: F.H. Walters

Department of Transportation
NASA/DOT Joint Office of
Noise Abatement
Washington, D.C. 20590
Attention: C. Foster

Federal Aviation Administration
Noise Abatement Division
Washington, DC 20590
Attention: E. Sellman AEE-120

Rohr Corporation
P.O. Box 1516
Chuyla Vista, CA 92012
Attention: James C. Fuscoe

TRW Equipment
TRW Inc.
23555 Euclid Ave.
Cleveland, Ohio 44117
Attention: I. Toth

Federal Aviation Administration
12 New England Executive Park
Burlington, MA 18083
Attention: Jack A. Sain, ANE-200

Curtiss Wright Corporation
Woodridge, NJ 07075
Attention: S. Lombardo
S. Moskowitz

AVCO/Lycoming
550 S. Main Street
Stratford, CN 06497
Attention: H. Moellmann

Williams Research Co.
2280 W. Maple Road
Walled Lake, MI 48088
Attention: R. VanNimwegen
R. Horn

Teledyne CAE, Turbine Engines
1330 Laskey Road
Toledo, OH 43612
Attention: R.H. Gaylord

Pratt & Whitney Aircraft Group/UTC
Government Products Division
P.O. Box 2691
West Palm Beach, FL 33402
Attention: B.A. Jones

Boeing Commercial Airplane Co.
P.O. Box 3707
Seattle, WA 98124
Attention: P.E. Johnson MS 9H-46
D.C. Nordstrom MS-73-01

Brunswick Corporation
2000 Brunswick Lane
Deland, FL 32720
Attention: A. Erickson

Delta Airlines, Inc.
Hartsfield-Atlanta International Airport
Atlanta, GA 30320
Attention: C.C. Davis

FluiDyne Engineering Corp.
5900 Olson Memorial Highway
Minneapolis, MN 55422
Attention: J.S. Holdhusen

Massachusetts Inst. of Technology
Dept. of Astronautics & Aeronautics
Cambridge, MA 02139
Attention: Mames Mar

Detroit Diesel Allison Div. G.M.C.
P.O. Box 894
Indianapolis, IN 46202
Attention: W.L. McIntire

The Garrett Corporation
AIResearch Manufacturing Co.
Torrance, CA 90509
Attention: F.E. Faulkner

The Garrett Corporation
AIResearch Manufacturing Co.
402 S. 36 Street
Phoenix, AZ 85034
Attention: Library

General Electric Co./AEG
1000 Western Avenue
Lynn, MA 01910
Attention: R.E. Nietzel

Pratt & Whitney Aircraft Group/UTC
Commercial Products Division
East Hartford, CT 06108
Attention: W. Gardner (3 copies)
I. Mendelson

Douglas Aircraft Co.
McDonnell Douglas Corp.
3855 Lakewood Boulevard
Long Beach, CA 90846
Attention: R.T. Kawai Code 36-41
M. Klotzsche 36-41

AIResearch Manufacturing Co.
111 South 34th Street
P.O. Box 5217
Phoenix, AZ 85010
Attention: C.E. Corrigan
(930120/503-4F)

American Airlines
Maint. & Engrg. Center
Tulsa, OK 74151
Attention: W.R. Neeley

Lockheed California Co.
Burbank, CA 91502
Attention: J.F. Stroud, Dept. 75-42
R. Tullis, Dept. 74-21

Grumman Aerospace Corp.
South Oyster Bay Road
Bethpage, NY 11714
Attention: C. Hoeltzer